

**A METHOD FOR RETAINING BETA PHASE  
IN THE CORE OF PLATES AND RODS  
OF TITANIUM ALLOYS**

*P. HERASYMENKO*

*J. WINTER*

*NEW YORK UNIVERSITY*

*NOVEMBER 1954*

MATERIALS LABORATORY

CONTRACT No. AF 33(616)-2259

PROJECT No. 7351

WRIGHT AIR DEVELOPMENT CENTER  
AIR RESEARCH AND DEVELOPMENT COMMAND  
UNITED STATES AIR FORCE  
WRIGHT-PATTERSON AIR FORCE BASE, OHIO

# *Contrails*

## FOREWORD

This report was prepared by New York University, under USAF Contract No. AF 33(616)-2259. The contract was initiated under Task No. 73510, (formerly RDO No. R615-11 SR-3c, "Titanium Metal and Alloys"), and was administered under the direction of the Materials Laboratory, Directorate of Research, Wright Air Development Center, with 1st/Lt E. F. Erbin acting as project engineer.

WADC TR 54-280

## ABSTRACT

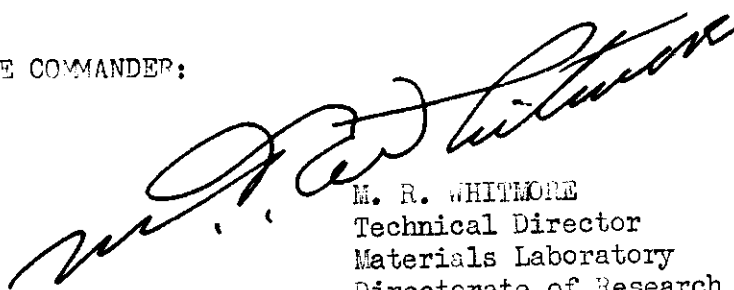
Twelve 1-kg ingots were prepared having the following nominal compositions: Ti-(6, 8, 10, 12%) Cr, Ti-3%Al-(6, 8, 10%) Cr and Ti- (6, 9, 12%) Mn. The ingots were forged to 1/2-inch and 3/4-inch square bars, which were heat treated using two-step quenching. Microstructures and hardness on the cross-section of bars were investigated.

Evidence is presented that soft beta can be retained in the center of bars and plates by step-quenching in alloys containing 12% Cr in the Ti-Cr series, 10% Cr in the Ti-3%Al-Cr series and 12% Mn in the Ti-Mn series. The outer layers of bars are considerably harder than the core after step-quenching.

## PUBLICATION REVIEW

This report has been reviewed and is approved.

FOR THE COMMANDER:



M. R. WHITMORE  
Technical Director  
Materials Laboratory  
Directorate of Research

# Contrails

## TABLE OF CONTENTS

	Page
Introduction. . . . .	1
I. Experimental Procedure. . . . .	2
II. Experimental Results . . . . .	3
A. Water-quenched Specimens. . . . .	3
B. Two-Step Quenching . . . . .	7
III. Discussion. . . . .	11

# Contrails

## LIST OF ILLUSTRATIONS

<u>Figure No.</u>		<u>Page No.</u>
Fig. 1	Hardness Distribution in 1/2-in. Square Specimens Water Quenched from 1000°C.	25
Fig. 2	Hardness Distribution in 3/4-in. Specimens Water Quenched from 1000°C.	26
Fig. 3	Photomicrograph of Ti-8% Cr. Center of 1/2-in. Bar. 100X	27
Fig. 4	Photomicrograph of Ti-10% Cr. Center of 1/2-in. Bar. 100X	27
Fig. 5	Photomicrograph of Ti-12% Cr. Center of 1/2-in. Bar. 100X	27
Fig. 6	Photomicrograph of Ti-3%Al-6%Cr. Center of 1/2-in. Bar. 100X	28
Fig. 7	Photomicrograph of Ti-3%Al-8%Cr. Center of 1/2-in. Bar. 100X	28
Fig. 8	Photomicrograph of Ti-6%Mn. Center of 1/2-in. Bar. 100X	28
Fig. 9	Photomicrograph of Ti-12%Mn. Center of 1/2-in. Bar. 100X	28
Fig. 10	Hardness Distribution in 1/2-in. Bars of Ti-6%Cr Alloy After Two-Step Quench.	29
Fig. 11	Hardness Distribution in 1/2-in. Bars of Ti-8%Cr Alloy After Two-Step Quench.	30
Fig. 12	Hardness Distribution in 1/2-in. Bars of Ti-10%Cr Alloy After Two-Step Quench.	31
Fig. 13	Hardness Distribution in 1/2-in. Bars of Ti-12%Cr Alloy After Two-Step Quench.	32
Fig. 14	Hardness Distribution in 1/2-in. Bars of Ti-Cr Alloys of Indicated Compositions After Two-Step Quench.	33
Fig. 15	Photomicrograph of Ti-10% Cr. Center of 1/2-in. Bar. 100X	34
Fig. 16	Photomicrograph of Ti-10% Cr. Center of 1/2-in. Bar. 100X	34
Fig. 17	Photomicrograph of Ti-12% Cr. Outer Layer of 1/2-in. Bar. 100X	34
Fig. 18	Photomicrograph of Ti-12% Cr. Center of 1/2-in. Bar. 100X	34

# Contrails

## LIST OF ILLUSTRATIONS (continued)

<u>Figure No.</u>		<u>Page No.</u>
Fig. 19	Hardness Distribution in 1/2-in. Bars of Ti-3%Al-6%Cr Alloys After Two-Step Quench.	35
Fig. 20	Hardness Distribution in 1/2-in. Bars of Ti-3%Al-8%Cr Alloys After Two-Step Quench.	36
Fig. 21	Hardness Distribution in 1/2-in. Bars of Ti-3%Al-10%Cr Alloys After Two-Step Quench.	37
Fig. 22	Hardness Distribution in 1/2-in. Bars of Ti-3%Al-Cr Alloys of Indicated Composition After Two-Step Quench.	38
Fig. 23	Hardness Distribution in 3/4-in. Specimen of Indicated Composition After Two-Step Quench.	39
Fig. 24	Photomicrograph of Ti-3%Al-8%Cr. Center of 1/2-in. Bar. 100X	40
Fig. 25	Photomicrograph of Ti-3%Al-8%Cr. Center of 1/2-in. Bar. 100X	40
Fig. 26	Photomicrograph of Ti-3%Al-10%Cr. Outer Layer of 1/2-in. Bar. 100X	40
Fig. 27	Photomicrograph of Ti-3%Al-10%Cr. Center of 1/2-in. Bar. 100X	40
Fig. 28	Hardness Distribution in 1/2-in. Bars of Ti-6%Mn Alloy After Two-Step Quench.	41
Fig. 29	Hardness Distribution in 1/2-in. Bars of Ti-9%Mn Alloy After Two-Step Quench.	42
Fig. 30	Hardness Distribution in 1/2-in. Bars of Ti-12%Mn Alloy After Two-Step Quench.	43
Fig. 31	Hardness Distribution in 1/2-in. Bars of Ti-Mn Alloys of Indicated Composition After Two-Step Quench.	44
Fig. 32	Photomicrograph of Ti-6%Mn. Center of 1/2-in. Bar. 100X	45
Fig. 33	Photomicrograph of Ti-9%Mn. Center of 1/2-in. Bar. 100X	45
Fig. 34	Photomicrograph of Ti-12%Mn. Outer Layer of 1/2-in. Bar. 100X	45
Fig. 35	Photomicrograph of Ti-12%Mn. Center of 1/2-in. Bar. 100X	45

## LIST OF ILLUSTRATIONS (continued)

<u>Figure No.</u>		<u>Page No.</u>
Fig. 36	Hardness in the Center of 1/2-in. Bars After Two-Step Quench versus Temperature of the First Quench.	46
Fig. 37	Effect of Composition on Hardness in the Center of 1/2-in. Rods After Single and Two-Step Quenching.	47
Fig. 38	The Titanium-Chromium Phase Diagram. (According to M. K. McQuillan.)	48
Fig. 39	The Free Energy, Activity Coefficient of Titanium and Hardness of Water Quenched Specimens as Functions of the Solute Content in Ti-Cr and Ti-Mn Alloys.	49
Fig. 40	Hardness in the Center and Outer Zone of 5/8-in. Rounds as a Function of the Temperature of the First Quench.	50
Fig. 41	Hardness (VHN), Diameter of Particles ( $d_{\Omega}$ and $d_{\alpha}$ ), and Density of Nucleated Particles ( $n_{\Omega}$ and $n_{\alpha}$ ) as Functions of the Temperature of the First Quench.	51
Fig. 42	Hypothetical Hardness Values in the Core of 1/2-in. Rods After Two-Step Quench as a Function of the First Quench Temperature for the Alloys of the Ti-3%Al-Cr and Ti-Mn Series.	52

# *Contrails*



It was found previously (1) that rods of Ti-3%Al-5%Cr alloy, water quenched from 1000°C, had a soft martensitic layer at the surface and a hard core of decomposed beta. However, when the same material was quenched from 1000°C into a lead bath at about 350°C, held there for 5-20 min, and finally quenched in water, the sequence of microstructures was reversed: the surface layer was a hard product of beta decomposition and the core had a soft martensitic structure. From a detailed study of these phenomena it was concluded that upon quenching from 1000°C to about 350°C, the transformation of beta to a mixture of phases having higher hardness starts from the surface of the rod and propagates slowly towards the center, the core remaining in the beta state for a considerable time. Final water quenching from 350°C leads to the transformation of beta to martensite in the core of the rods.

These observations seemed to make it probable that an increase in the content of alloying element might lead to a retention of beta in the core of rods or plates of sufficiently large cross-section when a two-step quench, as described above, was used.

Such a heat treatment could offer interesting possibilities of producing rods or plates that would be hard on the surface, due to the decomposition of beta, and soft in the core, where untransformed beta would be retained.

The aim of the present work was as follows:

(1) to verify the assumption that the retention of beta in the core of rods or plates is a general phenomenon which can occur in all titanium alloys containing a sufficient amount of beta-stabilizing alloying element;

(2) to find the lowest concentration of beta-stabilizing element at which beta could be retained in the core of rods and plates.

The nature of this study was exploratory, and it was undertaken to provide preliminary data for further, more detailed investigations of the mechanisms of the observed phenomena.

I. EXPERIMENTAL PROCEDURE

Two-pound ingots of 10 alloys of the following compositions were prepared:

<u>Group</u>	<u>%Al</u>	<u>%Cr</u>	<u>%Mn</u>
Ti-Cr	-	6	-
	-	8	-
	-	10	-
	-	12	-
Ti-Al-Cr	3	6	-
	3	8	-
	3	10	-
Ti-Mn	-	-	6
	-	-	9
	-	-	12

The titanium sponge used in the preparation of ingots was of BHN-129.

In order to insure homogeneity in the final ingots, twenty 50-g buttons for each composition were melted twice in an arc-furnace. These buttons were then consolidated by remelting in a 2-lb arc-furnace to form a 2-lb ingot. The ingots were machined smooth and forged into square bars. One end of each bar was 3/4 in. square for a length of about 3 in.; the rest of the bar was 1/2 in. square. The forging temperature was about 1000°C.

For heat treatment, specimens of 1-in. length were cut from 1/2-in.-thick rods, and those of 1-1/2-in. length from the 3/4-in. thick ends. To insure symmetrical distribution of hardness from the surface to the center of the rods, a small hole was drilled near one end of each specimen into which the bent end of a long steel wire was inserted. This enabled the rapid withdrawal of specimens from the furnace and submersion in a lead bath or water in a vertical position.

The heat treatments used were:

- (1) solution treatment for 20 min at 1000°C followed by water quench;
- (2) solution treatment for 20 min at 1000°C, first quenching in a lead bath at temperatures of 330, 350, 375, 400 and 450°C, isothermal holdings at these temperatures for 5 or 10 min, followed by water quench.

After heat treatment, the specimens were cut in two halves perpendicularly to the rod axis. One surface of the cut served for the measurement of hardness distribution and the other for the study of microstructures. Hardness measurements were made on the cross section of bars in two directions: along the diagonal and along the line joining the centers of two opposite sides. The indentations were made at about 1 mm intervals. In the case of water-quenched specimens, only five indentations were made on the cross-section along the line joining two opposite sides.

## II. EXPERIMENTAL RESULTS

### A. Water-Quenched Specimens:

The distribution of hardness in water-quenched specimens is shown in the diagram of Fig. 1.

*Continued*

Alloys of the Ti-Cr system show comparatively high hardness both near the surface and in the center at 6 and 8% Cr. Alloys with 10 and 12% Cr have low hardness in the whole cross-section.

Alloys of the Ti-3%Al-Cr series had low hardness in the whole cross-section for all chromium contents investigated. Hardness tends to increase from 6 to 10% Cr content.

Typical microstructures of water-quenched Ti-Cr alloy bars are shown in Fig. 3. The microstructure in all cases was practically the same in the center as in the outer layers of bars. No martensite was found in the outer layer, even in the alloy with 6% Cr. In the core of bars with 8% and 10% Cr, slip lines were observed which in some crystals were curved. These lines indicate that the grains in the core were subject to deformation stresses during cooling. At all chromium contents one could find grains which had only a very small amount of precipitate beside the grains with almost the complete cross-section covered by fine precipitate.

Areas with fine precipitate were increasingly darker with increasing chromium content and were somewhat darker at the center than in the outer layer. A similar tendency was observed in other alloy series.

The Ti-3%Al-6%Cr bar had a typical martensitic structure in the whole cross-section (Fig. 6). Bars with 3%Al-8%Cr and 3%Al-10%Cr had structures similar to those observed in the Ti-Cr series, except that no sharp slip markings were detected. Very fine precipitate was visible in most grains but it was distributed evenly over the cross-section of individual grains.

Hardness distribution on the cross section of water-quenched 3/4-in.-square bars of Ti-3%Al-8%Cr and Ti-3%Al-10%Cr alloys is shown in the diagrams of Fig. 2. The hardness values in this case are practically the

same as in 1/2-in. bars. The microstructure was retained beta with very fine precipitate, similar to the 1/2-in bars.

These almost carbon-free Ti-Al-Cr alloys do not develop a hard core on water quenching, as was observed in the 5/8-in bars of the commercial 3%Al-5%Cr alloys. Carbon, and probably nitrogen, present in the commercial alloy accelerated the decomposition of beta, so that even water-quenched bars had partially transformed cores.

In the Ti-Mn series, specimens with 6% Mn had high hardness (VHN~400), and the structure was typically martensitic with indications of fine precipitate in the original beta matrix (Fig. 8). Alloys with 9 and 12% Mn had beta grains with very fine precipitate ("pepper") in the grains (Fig. 9). The 12% Mn alloy had a smaller amount of precipitate.

It was impossible to judge from the microstructure of water-quenched specimens whether the original beta grains with fine precipitate had retained beta phase; the nature of the precipitate could not be determined.

In the Ti-Cr series, the high hardness in the center of water-quenched specimens containing 6 and 8% Cr might be due to the decomposition of beta between the martensitic needles. The low hardness in specimens with 10 and 12% Cr seems to indicate that a large proportion of beta remained untransformed and that the precipitate observed in the beta matrix does not harden the matrix.

In the Ti-Al-Cr series, the water-quenched specimens had low hardness at all chromium contents investigated. It was observed previously that transformation in 1/2-to 1/in. rounds of commercial 3%Al-5%Cr alloy is very sensitive to the presence of interstitials. The presence of nitrogen and oxygen can prevent the formation of the outer martensitic layer during water quenching. The fact that our water-quenched 3%Al-6%Cr alloy had very

# Conclusions

low hardness from the surface down to the center of the rod indicates that the content of nitrogen (from the sponge and picked up during melting) was fairly low. Since the alloys in the Ti-Cr series were made from the same sponge, it is probable that the high hardness in the center of water-quenched 6 and 8% Cr specimens reflects the inherent behavior of the Ti-Cr system in this range of chromium contents. Independent supporting evidence in favor of this conclusion can be derived from the data on the Ti-Cr phase diagram published by (Mrs.) M.K. McQuillan<sup>(2)</sup> after our present investigation was completed. This evidence will be discussed in more detail at the end of this report. Meanwhile, it will suffice to state that a relative tendency of beta to nucleate alpha phase appears to be greater in the interval from 5 to 8% Cr than at lower or higher chromium contents.

In the presence of 3% aluminum, the beta phase can be more easily supercooled even at 6 and 8% Cr, so that it does not decompose on water quenching in a manner such as was observed in Ti-Cr alloys without aluminum. A large proportion of beta phase is retained by water quenching 1/2 in. and 3/4 in. specimens of Ti-3%Al-Cr alloys, as was proved by the following observations: the average hardness in the core of a 3/4-in. bar of Ti-3% Al-8% Cr alloy was VHN=285; on subsequent reheating to 450°C for one hour, the core hardness in the same bar increased to VHN=439 (average of 5 readings).

In the Ti-Mn series, rods containing 6% Mn had comparatively high hardness after water quenching, and in this case the beta matrix between the martensitic needles probably decomposed simultaneously with or very soon after the formation of martensite. At higher contents of manganese no martensite needles were observed and a considerable amount of beta was retained, as can be judged from the low hardness of water-quenched specimens with 9 and 12% Mn.

## B. Two-Step Quenching:

The heat treatment of bars was as follows: solution treatment at 1000°C for 30 min, quenching in a lead bath at temperatures of 330, 350, 375, 400 and 450°C, isothermal holding at these temperatures for 5 or 10 min, followed by water quenching.

### 1. Ti-Cr Series:

Hardness data for these alloys are recorded in Figs. 10-14. Bars from the alloys with 6, 8 and 10% Cr had practically constant hardness across the whole cross-section. Maximum hardness was developed in all cases when specimens were isothermally held in the lead bath at 350°C for 5 min. The alloy with 12% Cr showed a sharp decrease in hardness in the center of bars in a narrow range of lead-bath temperatures between 350 and 375°C (Fig. 13). Specimens of the 12% Cr alloy quenched at 375 and 400°C had low hardness in the core and higher hardness near the surface.

The microstructure in all cases showed the beta grain boundaries with fine precipitate. The microstructures had similar features at all chromium contents and there was no correlation with hardness (Figs. 15-18). Generally, the areas with fine precipitate appear darker when quenched at higher lead-bath temperatures than at lower temperatures. It was observed that areas with fine precipitate stand slightly in relief over the areas in the same grain that apparently have no precipitate. Further, it was found that quite often the precipitate outlined the contours of some sort of lenses in the matrix of grains. These phenomena are not confined to one particular alloy or a particular alloy series, and no certain explanation has yet been found.

The presence of a very fine precipitate in the beta matrix in most two-step quenched samples led to a supposition that alloys absorbed

# Contrails

hydrogen during some stage of melting or heat-treatment, and that at least part of the precipitate was composed of hydride particles. The microstructures were examined in late stages of this study when a large number of samples from the Ti-Cr and Ti-3% Al-Cr alloy series were heat treated. It was not excluded a priori that the presence of hydrogen could also affect the response of alloys to heat treatment. In order to decrease such effects of hydrogen, the remaining samples were annealed in vacuo at 600°C for two hours and then heat-treated; several new samples of Ti-Cr and Ti-3%Al-Cr alloys were also annealed in vacuo and then heat treated in the same way as specimens treated in vacuo. The microstructure of initially vacuum-treated bars was not essentially different from that of non-treated specimens. Also, with a few exceptions, the hardness of vacuum-treated specimens did not differ from that of non-treated samples. However, it must be pointed out that both the temperature (600°C) and time (2 hours) of de-hydrogenation could have been insufficient for a good removal of hydrogen, and the problem of the effect of hydrogen on microstructure and hardness must be left open for further experiments.

In order to obtain qualitative information on the amount of beta retained in the soft core of Ti-12% Cr rods after the two-step quench, these specimens were subsequently annealed at 500°C for 2 hr, and hardness measurements were made in the center. Any retained beta should decompose during this anneal and the hardness should increase. The results were as follows:

<u>Alloy</u>	<u>Lead bath temp., °C</u>	<u>VHN after 2 step quench</u>	<u>VHN after subsequent 2 hr anneal at 500°C</u>	<u>Hardness increase</u>
Ti-12%Cr	375	300	376	+76
	400	305	367	+62



*Controls*

Hardness after annealing at 500°C did not increase to the high level (VHN ~475) obtained with the same alloy isothermally treated at 350°C. This fact makes it probable that annealing at 500°C for 2 hr produced an overaging.

2. Ti 3%Al-Cr Series:

Hardness measurements for this series are recorded in Figs. 19-23. Hardness tends to increase with increasing temperature of the lead bath. Alloys with 6 and 8% Cr have practically constant high hardness through the whole cross-section of rods. The alloy with 10% Cr has low hardness in the center as well as at the surface at 330 and 350°C. At higher temperatures of the lead bath the core was soft and the outer layers fairly hard.

The microstructures in all cases showed beta grain boundaries with a fine precipitate. As in the foregoing series, no definite correlation could be found between microstructure and hardness. Typical examples of the microstructures are shown in Figs. 24-27. To obtain qualitative indications of the amount of beta retained in rods after two-step quenching, 1/2-in. specimens were aged at 500°C for 2 hr and hardness was determined in the core. The following table gives the results:

<u>Alloy</u>	<u>Lead bath temp., °C</u>	<u>VHN (avg) after 2-step quench</u>	<u>VHN (avg) after subsequent 2-hr anneal at 500°C</u>	<u>Hardness Increase, Δ VHN</u>
3%Al-6%Cr	350	375	419	+44
3%Al-6%Cr	400	405	419	+15
3%Al-8%Cr	400	465	430	-35
3%Al-10%Cr	330	300	415	+115
"	350	295	422	+127
"	375	275	419	+144
"	400	305	433	+128

*Continued*

One 3/4-in. specimen of 3%Al-10%Cr alloy first quenched at 375°C had, in the core, the average hardness VHN-290. After aging at 450°C for 1 hour, hardness increased to 422.

The hardness of 3%Al-6%Cr specimens increased slightly on aging, indicating that the decomposition of beta to a hard mixture was almost complete during the first quench step. The small decrease of hardness in 3%Al-8%Cr specimens indicates over-aging.

The large increase of hardness in all specimens of 3%Al-10%Cr alloys indicates that a large amount of beta was retained after the two-step quench. The rate of decomposition of beta to a hard mixture on annealing at 500°C seems to be higher than in the case of 12% Cr alloy.

### 3. The Ti-Mn Series:

The hardness measurements for this series are recorded in Figs. 28-31. The Ti-6%Mn specimens have high hardness at 330, 350 and 375°C; specimens quenched at 400 and 450°C show a tendency towards hardness increase with increasing temperature of the lead bath up to 400°C; at 450°C the hardness considerably decreases.

The Ti-12%Mn rods were considerably softer in the center than the alloys with lower manganese contents; the outer layers, however, are harder than the core.

Typical microstructures are shown in Figs. 32-35. Beta grain boundaries and fine precipitate within the grains are visible. Again, there is no definite correlation between microstructure and hardness. Even the softest parts in the center of bars with 12% Mn have more or less abundant, finely precipitated particles. A few short-line markings were observed in some grains in the core of the Ti-6%Mn bars, and slip

# Conclusions

markings extending over the whole cross-section of grains in the core of bars with 12%Mn (Fig. 35). This can be taken as a direct indication of stresses in the core developed during cooling to 400°C. Although the cooling rate in this case was less severe than on water quenching from 1000°C, the stresses were sufficiently large to deform the material in the core.

To obtain qualitative information on the amount of beta retained in rods after the two-step quench, several Ti-12%Mn specimens were annealed at 550°C for two hours and hardness was determined in the core. The results were as follows:

<u>Alloy</u>	<u>Lead bath Temp., °C</u>	<u>VHN (avg) after 2-step quench</u>	<u>VHN (avg) after subsequent 2-hr anneal at 500 °C</u>	<u>Hardness increase, ΔVHN</u>
Ti-12%Mn	330	325	376	+51
	350	370	382	+12
	375	330	362	+32
	400	305	388	+82

The hardness increase in this alloy is not so great as in the Ti-3%Al-10%Cr alloy, but this may be due either to the slowness of the beta decomposition or to overaging of the Ti-12%Mn alloy at 500°C.

## DISCUSSION

The results of the present study are summarized in Figs. 36 and 37. The hardness in the center of 1/2-in. square rods of the alloys studied is plotted in the diagrams, Fig. 36, as a function of the temperature of the lead bath. Hardness in the center of rods either directly water quenched or first quenched to 400°C is shown in Fig. 37 as a function of composition. Some of these observations can be interpreted by

# Contrails

considering the results of a new study on the titanium-rich portion of the titanium-chromium diagram published by (Mrs.) M. K. McQuillan when the final version of this report was being prepared. The beta-transus curve in her work (see Fig. 38) shows two inflections: one at about 4.5%Cr, another at about 7-8%Cr. These findings were analyzed by one of the present authors (P.H.) in a written discussion submitted recently to the Journal of the (British) Institute of Metals.

Dr. A. D. McQuillan has shown previously (3) that the  $\beta/(\alpha+\beta)$  boundaries for binary alloys containing up to 5 atomic percent of Cr, Mn, Co and Ni follow a course very close to the idealized boundary for the ideal solid solution in equilibrium with alpha phase containing negligible amounts of solute atoms. In the titanium-iron system, the  $\beta/(\alpha+\beta)$  boundary is higher than the idealized one, and therefore the beta phase should considerably deviate from the behavior of ideal solid solutions.

The course of the  $\beta/(\alpha+\beta)$  boundary for the Ti-Cr system established by Mrs. McQuillan indicates that the behavior of the beta phase in this case shows a deviation from ideality of a solid solution at chromium contents above about 4.5% Cr. The following thermodynamic analysis of the  $\beta/(\alpha+\beta)$  boundaries for titanium-chromium and titanium-iron systems may be of general interest to the theory of titanium alloys. The data taken for this analysis were as follows:

- (1) heat capacities of pure alpha and beta titanium:

$$\alpha\text{Ti}^{(4)}: C_p = 5.9 \times 2.96 \times 10^{-3}T$$

$$\beta\text{Ti}^{(5)}: C_p = 7.525$$

- (2) heat of  $\alpha-\beta$  transformation<sup>(6)</sup>

$$\Delta H^{0882.5^\circ\text{C}} = 678 \text{ cal/g-at.}$$

# Contrails

- (3) the solubility of chromium and iron in the alpha phase is assumed negligibly small.

From these data, the free energy of alpha titanium relative to beta was found to be:

$$\Delta F^{\circ} = 824 + 9.040T - 2.303 \times 1.625 T \log T + 1.48 \times 10^{-3} T^2$$

Applying this equation to the  $\beta / (\alpha + \beta)$  boundaries as found by Dr. A.D. McQuillan and Mrs. McQuillan for titanium-iron and titanium systems, the activities and activity coefficients of titanium in beta solid solutions at temperatures of the  $\beta / (\alpha + \beta)$  boundaries have been calculated for the range of concentrations investigated by both authors. The course of free energies and of activity coefficients of titanium in these two systems are shown in upper diagrams of Fig. 39.

It is seen that the activity coefficient of titanium in the beta phase of titanium-chromium alloys is practically equal to unity up to about 4.5% Cr: the beta phase can thus be regarded in this composition range as a nearly ideal solution. Above 4.5 at.% Cr, the activity coefficient rapidly increases and attains a maximum value,  $\alpha_{Ti} = 1.016$  at about 7 at.% Cr. In the interval from 7 to 9 at.% Cr the activity coefficient decreases below unity. In the titanium-iron system the activity coefficient of titanium in the beta phase increases above unity at the smallest additions of iron.

The value of the activity coefficient of titanium in beta phase can be taken as an approximate measure of the tendency to alpha precipitation. Alloys having a low activity coefficient are more likely to retain beta on quenching from high temperatures than alloys with  $\alpha_{Ti} > 1$ . In the titanium-chromium system, one would expect that the tendency to precipitate alpha should be higher in the range from 4.5

to 8 at.% Cr, than at chromium contents lower than 4.5 at.% or higher than 8 at.%. Actually beta transforms to martensite at low chromium contents, but this reaction, being a diffusionless process, involves only a minor displacement of atoms in the lattice and not the formation of two new phases by a long-distance diffusion process.

It was observed that the martensitic phase in those cases where its formation was not accompanied or followed by the nucleation and growth of alpha particles has a low hardness comparable to that of retained beta. The formation of a fine precipitate of alpha in the beta matrix or in the martensitic structure becomes evident from a considerable increase of hardness, although in many cases alpha cannot be detected metallographically.

The above conclusion that alloys having  $a_{Ti} > 1$  should show a greater tendency to nucleate alpha is fully confirmed by experimental data.

The lower diagram in Fig. 39 shows that 1/2-in. square rods of titanium-chromium alloys, when quenched from 1000°C in water, have an increased hardness in the range between 5 and 9 at.% Cr with a maximum at about 7 at.% Cr, which corresponds to the maximum on the curve of the activity coefficient for this system. The hardness measurements by Worner (7) on thin specimens of titanium-iron alloys quenched in water from 950°C show that the tendency for the nucleation of alpha becomes evident in thinner sections and at a much lower content of alloying element than in titanium-chromium alloys. This fact also conforms with the course of the activity coefficient of titanium in Ti-Fe alloys.

An increased activity of titanium in beta phase at certain

# Conclusions

compositions and the corresponding increase in the tendency to nucleate alpha phase can be explained mechanistically by assuming that titanium atoms at these compositions form clusters in the beta phase, and therefore alpha phase can easily nucleate on cooling. Clustering of similar atoms corresponds to a high degree of disorder in solid solutions (disorder higher than in ideal solutions, where the distribution of atoms is entirely random).

The above discussion explains reasonably well why the hardness of water-quenched rods in the Ti-Cr system attains a maximum in the range from 6 to 8 percent chromium. The increased hardness is thus due to hardening by submicroscopic precipitation of alpha particles. A similar explanation can also be applied to Ti-Mn alloys, which attain maximum hardness on water quenching at about 6% Mn.

A thermodynamic analysis of Ti-3%Al-Cr alloys could not be made because the situation in this system is more complex than in the binary Ti-Cr, Ti-Fe and Ti-Mn systems. However, the fact that water quenching of 1/2- and 3/4-in. specimens of Ti-3%Al-Cr alloys produces soft material with a considerable proportion of retained beta can be taken as an indication that the beta phase possesses in this case a higher degree of ordering than in the Ti-Cr system in spite of the fact that additions of aluminum raise the beta-transus boundary.

As is seen from Fig. 37, the maximum of the hardness in the Ti-Cr, Ti-3%Al-Cr and Ti-Mn systems displaces towards higher contents of alloying element when the rate of cooling from 1000°C decreases, i. e., the rods quenched in a lead bath at 400°C have maximum hardness at a higher content of alloying element than rods quenched in water. It seems

# Contrails

possible that this shift in the position of maximum hardness towards higher contents of alloying element in rods quenched to 400°C may be due to partial precipitation of compounds during cooling ( $TiCr_2$ ,  $TiMn$ ) as a result of which the composition of the remaining beta phase displaces towards lower contents of alloying element where the beta phase is less stable. However, no conclusive evidence can be adduced to support this supposition.

For further interpretation, the results of this study must be correlated with the findings of our previous investigation on the two-step quenching of rods of 3%Al-5%Cr alloy (1). The 5/8-in. rounds of this alloy were solution treated at 1000°C for 30min, quenched first in a liquid metal bath at temperatures ranging from 150 to 600°C, held there for 10 or 20 min and finally quenched in water. The dependence of hardness in the core and surface layers of the rods on the temperature of the liquid-metal bath is shown in Fig. 40 for two heats of this alloy. The curves show two hardness maxima for the center of rods. In the temperature range near the minimum hardness the center of rods had martensitic structure, and it was proved experimentally that martensite formed during the final water quench from beta which was retained in the core at the temperature of the liquid metal bath. At temperatures on both sides of the minimum hardness the rate of beta decomposition was higher than at the minimum. The existence of two hardness maxima suggests that there are probably two mechanisms of isothermal beta decomposition in the center of rods at two temperatures: the first at around 500°C and the second at about 200-250°C.

In the previous report (1) the processes occurring in these



*Control*

two temperature regions were described as a decomposition of beta to beta prime. It is recalled that beta prime was defined as a structure having high hardness and showing original beta grain boundaries with or without visible fine precipitate in the beta matrix. This definition of the beta prime structure is obviously unsatisfactory to describe rationally the occurrence of two maxima in the hardness-temperature curves for the core of two-step quenched rods.

In the following discussion it is assumed that there are two distinct mechanisms which lead to the occurrence of hardness peaks in the curves of Fig. 40.

- (1) decomposition of beta to alpha plus beta in the region above about 450°C;
- (2) decomposition of beta to some intermediate phase, possibly the omega phase discovered by workers at Battelle Memorial Institute.

The nature of the second reaction mechanism is at present rather obscure.

It should be recalled that for small specimens (1/8-in. thick or less) the curve shows only one maximum of hardness (see curve in upper diagram of Fig. 39). However, a careful examination of experimental points indicates that there is a probability for the occurrence of a change in the slope of the hardness curve at about 630°C (point C at VHN ~ 400).

To explain the difference between small and large specimens, let us consider the probable cause of hardness in two-step quenched specimens. As a rough approximation, the hardness caused by both reaction mechanisms is regarded as due to precipitation hardening. Hardness is considered as a function of the number of particles of the new phase (density of nuclei) and of the size of the new-phase particles. This function is assumed to be represented by the following formula:

$$\text{VHN} = \frac{n}{d} + \text{constant}$$

where  $n$  is the number of particles nucleated in a given time, and  $d$  is the diameter of particles.

The assumed size of particles (in arbitrary units) is plotted in the dashed curves in Fig. 41 for the two reaction mechanisms. The diameter below which the particles cannot be resolved under the microscope is indicated by a horizontal line AB. The size of alpha particles is shown to increase exponentially with increasing temperature. The assumption is based on the fact that these particles become visible under the microscope at temperatures above about 650°C, and form a Widmanstatten pattern which is increasingly better developed as the temperature of the metal bath increases. The size of omega particles is assumed to be very small and almost independent of temperature. These particles cannot be resolved under the microscope. In the same diagram, Fig. 41, the observed hardness of small specimens is plotted as a solid curve. Using the above formula, the number of nucleated particles ( $n$ , in arbitrary units) was calculated from the observed hardness values and the assumed diameter of particles. It is seen that the  $n$ -values form two distinct curves with maxima at 400°C for omega particles and at 700°C for alpha particles. There is a very small overlap of the two curves.

Starting from this deduction, the shape of the observed hardness curves for larger specimens can be interpreted as follows:

The hardness curves of surface layers of bars in Fig. 40 show a very pronounced change in slope when, on going from higher to lower temperatures, hardness reaches about 400 VHN. Quenching to lower temperatures produces only a small increase in hardness down to about 300°C.

The fact that the surface hardness of rods in the range from 500 to 300°C does not increase to the high values observed with small specimens indicates that the nucleation of omega phase is greatly delayed in the surface layers. The delay is due mainly to the fact that large specimens have a higher heat content than small specimens: on immersion of rods in a lead bath at, say, 350°C, the surface layers remain at temperatures above 400°C for a longer time than small specimens. Consequently, the surface layers have enough time to form a fine precipitate of alpha particles and to attain the highest hardness value of approximately 400 VHN for this reaction mechanism. Due to the formation of alpha particles, the remaining beta phase is enriched with the alloying element to such an extent that it becomes very stable and the nucleation of omega phase is suppressed or delayed.

Only a large supercooling of surface layers leaves sufficient amounts of un-enriched beta, so that the nucleation of omega phase can proceed rapidly, thus leading to a further increase in hardness of the surface layers. At metal bath temperatures lower than about 250°C, the supercooling becomes so large that the rate of omega nucleation decreases again, and hardness decreases also.

For the explanation of the hardness curve in the center of rods, an additional assumption is necessary. When quenched in a lead bath at 500°C, beta in the center can decompose to alpha, and hardness increases to a maximum. The decomposition, however, can be delayed by stresses induced in the core by cooling, and by volume changes accompanying the decomposition in the outer layers. The data available at present are not sufficient to describe quantitatively the nature of

stresses in the core of rods during the first quench treatment, and further measurements are necessary. The inspection of the diagrams in Fig. 40 reveals a probably significant fact, that the decomposition of beta in the center becomes slower when the hardness in the outer layers of rods approaches  $VHN \sim 400$ , which occurs at bath temperatures below  $500^{\circ}C$ .

At temperatures lower than about  $600^{\circ}C$ , beta in small specimens decomposes rapidly to omega and at about  $450^{\circ}C$  hardness increases to the maximum value of  $VHN=500$ . No such hardness increase is observed in the center of rods at temperatures below  $450^{\circ}C$ . This indicates that it is mainly the nucleation of omega phase that is suppressed by the stresses in the center of rods. In terms of the explanation proposed in our diagram, Fig. 41, this would indicate that the curve of omega nucleation is displaced by internal stresses in the center of rods towards lower temperatures.

The qualitative picture derived above can be taken as a working hypothesis only, since little is known of the nature and mechanism of formation of the intermediate phase, which is assumed here to be omega phase.

The results of the present study were summarized in Figs. 36 and 37.

Let us consider first the alloys of the Ti-3%Al-Cr series (Fig. 36). Hardness in the core of 3%Al-8%Cr alloy increases with increasing bath temperature up to  $400^{\circ}C$  and then decreases. This course of the curve suggests that low hardness in the center could be attained at bath temperatures below  $300^{\circ}C$ . Hardness in the core of rods of the 3%Al-6%Cr alloy is lower than that of the 3%Al-8%Cr alloy, but shows a similar

*Contrails*

trend, maximum hardness probably being at  $450^{\circ}\text{C}$ . Lower values of hardness were observed in the commercial 3%Al-5%Cr alloy, with a maximum at about  $500^{\circ}\text{C}$ . Thus, it can be concluded that the observed hardness values in the 3%Al-6%Cr and 3%Al-8%Cr alloys correspond to the region near the first maximum in Fig. 40. A retention of beta in the core of rods of 3%Al-6%Cr and 3%Al-8%Cr alloys can be predicted to occur below  $300^{\circ}\text{C}$  (in the region between 200 and  $300^{\circ}\text{C}$ ). This prediction could not be confirmed because the liquid-metal bath for these low temperatures was not available.

Hardness in the center of rods of the 3%Al-10%Cr alloy is very low at all bath temperatures, indicating that beta phase at this composition is much more stable than at lower chromium contents. It is interesting to note that the 3%Al-10%Cr alloy has a soft core and hard surface layers when quenched to  $375$  and  $400^{\circ}\text{C}$ . At lower bath temperatures, ( $350$  and  $330^{\circ}\text{C}$ ) the hardness is practically the same in the center and in the surface layers, thus showing that super-cooling of the surface layers was sufficiently rapid to retain beta almost completely.

The middle diagram in Fig. 37, where hardness in the core is plotted against the content of chromium, shows that the 3%Al-8%Cr alloy at a lead-bath temperature of  $400^{\circ}\text{C}$  has the maximum hardness. Extrapolation into the region of the commercial 3%Al-5%Cr alloy gives for the latter a hardness of the same magnitude as was actually observed in our previous study. (1)

The results for the Ti-3%Al-Cr series seem to indicate that the rate of alpha nucleation increases with increasing content of chromium up to 8% Cr and then rapidly decreases, so that at 10% Cr it becomes small.

# Conclusions

In the Ti-Cr series, core hardness vs temperature curves (Fig. 36) have a maximum at about 350°C. Soft core and comparatively hard surface layers were found in the Ti-12%Cr alloys quenched to 375 and 400°C (see Fig. 13). The latter alloy is very sensitive to small variations in the temperature of the lead bath: quenching to 350°C produced a high hardness in the whole cross-section of rods.

In the Ti-Mn series, the conditions appear to be similar to those observed with Ti-3%Al-Cr alloys (see lower diagrams in Fig. 38 and 39). Therefore, it is reasonable to assume that the observed hardnesses correspond to the first maximum of Fig. 41, i.e., to the region of alpha nucleation. It can be expected that the region of beta stabilization in the core of rods will be found at lead-bath temperatures below about 300°C. Again, the confirmation of this conclusion must be left to future experiments.

Soft core and hard surface layers were obtained with rods of 12%Mn alloy quenched above 375°C. A similar tendency is shown by the alloys with 6% Mn at higher quenching temperatures and by alloys with 9%Mn. Generally the hardness curves for manganese are more erratic than those for other alloys. This may possibly be due to the variation in the manganese content in the cross-section of the original ingot caused by local vaporization of manganese during arc-melting.

Summarizing this preliminary study, it can be said that two-step quenching can produce soft core and hard surface layers in rods of different chemical composition, and therefore this method can be applied generally. In the present study this result was obtained with Ti-12%Cr, Ti-3%Al-10%Cr and Ti-12%Mn alloys by first quenching at 400°C, holding

at this temperature for 5 min, and finally quenching in water.

An examination of experimental results indicates the strong probability that similar results can be obtained also with alloys having a lower content of alloying element (e.g. Ti-3%Al-6%Cr, Ti-3%Al-8%Cr, Ti-6%Mn and Ti-9%Mn) by using liquid-metal baths in the range from 200 to 300°C for the first quench step.

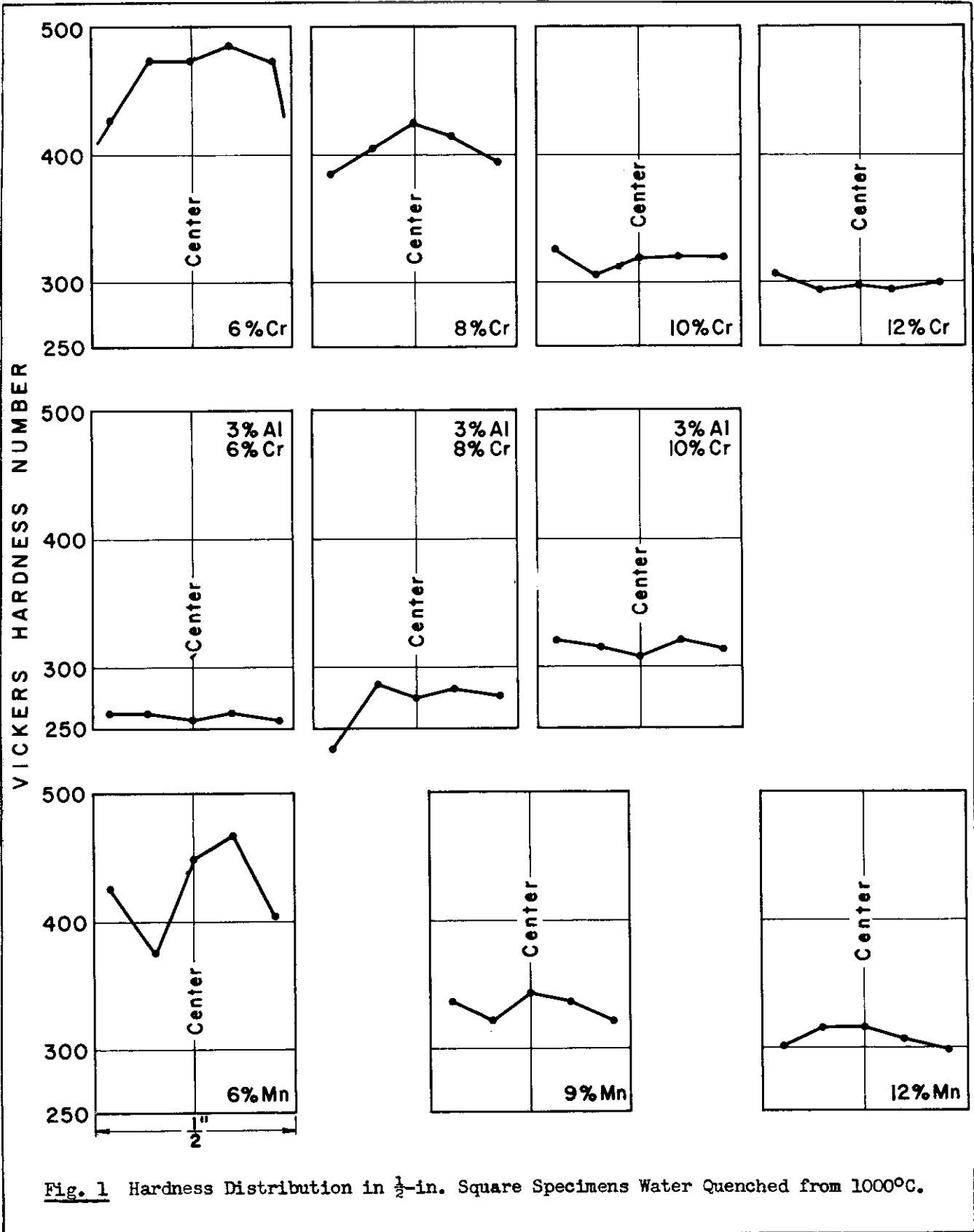
The hypothetical course of the hardness in the center of rods or plates after two-step quenching is indicated in Fig. 42 for Ti-3%Al-Cr and Ti-Cr alloys. A prediction of similar curves for Ti-Cr alloys is less certain and was not attempted. Low hardness in the center of bars for alloys with high alloy content (12%Cr, 3%Al-10%Cr and 12%Mn) was interpreted here as due to the retention of beta, although the microstructural evidence is not conclusive. The main reason for this interpretation is the fact that hardness in the core of these alloys increases substantially on aging.

## REFERENCES

1. P. Herasymenko and H. Margolin: "Heat Treatment of Ti-Al-Cr Alloys," Final Report to Bureau of Aeronautics, Navy Dept, on Contract NOa(s)53-018-C
2. M. K. McQuillan: J. Inst. Metals (1954), 82, p.433
3. A. D. McQuillan: J. Inst. Metals (1952), 80, p.363
4. O. Kubaschewski and E. L. Evans: "Metallurgical Thermochemistry,"1951, London (Butterworth-Springer, Ltd.)
5. F. M. Jaeger, E. Rosenbohm and R. Fonteyne: Proc. Acad. Amsterdam(1936),39,p.445; Rec. Trav. Chim.(1936),55,p.618
6. A. D. McQuillan: Proc. Roy. Soc. 1950, A 204, p.309
7. H. W. Worner: J. Inst. Metals(1952), 80, p.213



# Contrails



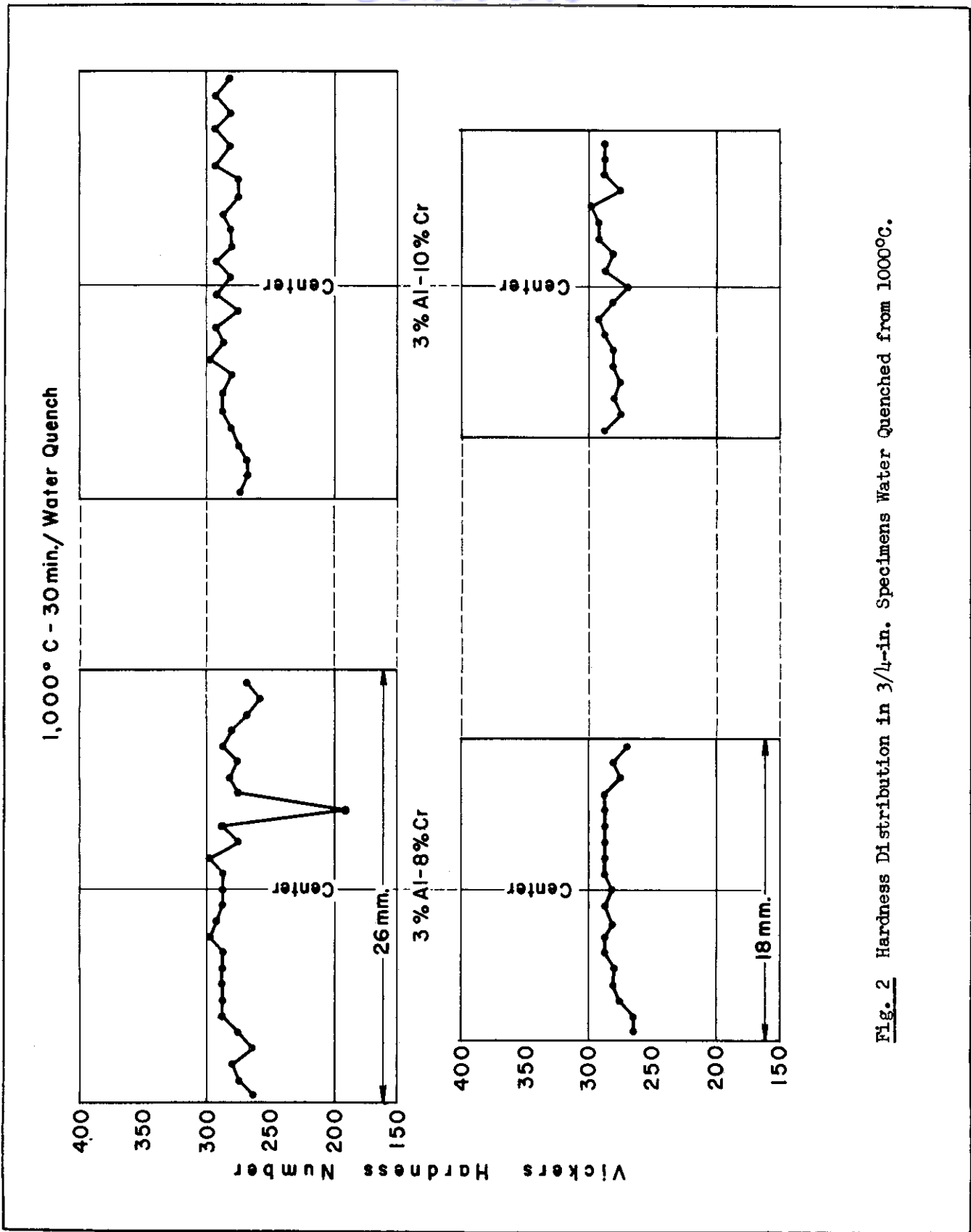
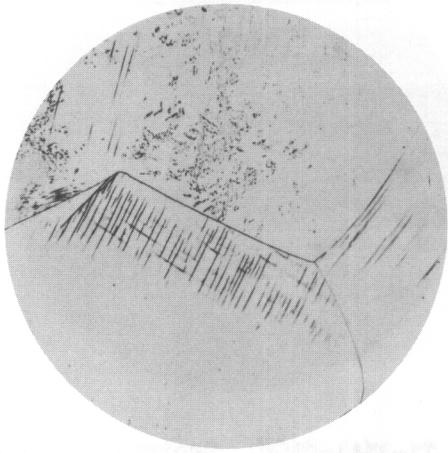
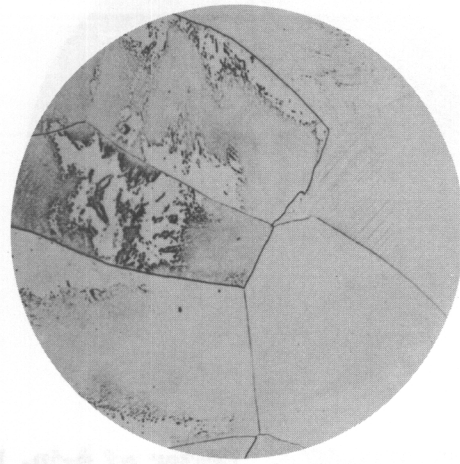


Fig. 2 Hardness Distribution in 3/4-in. Specimens Water Quenched from 1000°C.

# Contrails



**Fig. 3** Ti-8%Cr. Center of  $\frac{1}{2}$ -in. Bar.  
1000°C-20min/W.Q. VHN=425. 100X.



**Fig. 4** Ti-10%Cr. Center of  $\frac{1}{2}$ -in. Bar.  
1000°C-20min/W.Q. VHN=320. 100X.

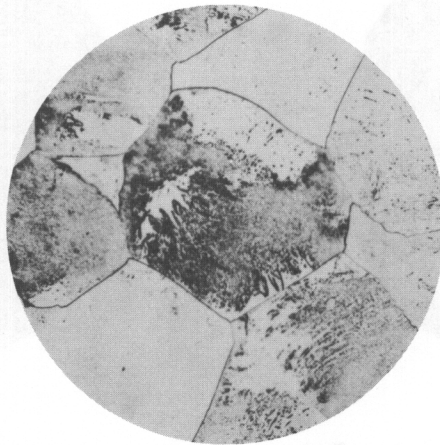


**Fig. 5** Ti-12%Cr. Center of  $\frac{1}{2}$ -in. Bar.  
1000°C-20min/W.Q. VHN=295. 100X.

10 ML. GLYCERINE, 10 ML. CONC HNO<sub>3</sub>, 10 ML. HF, ETCH

WADC TR 54-280

-27-

# Contrails



**Fig. 6** Ti-3%Al-6%Cr. Center of  $\frac{1}{2}$ -in. Bar.  
1000°C-20min/W.Q. VHN=260 100X.

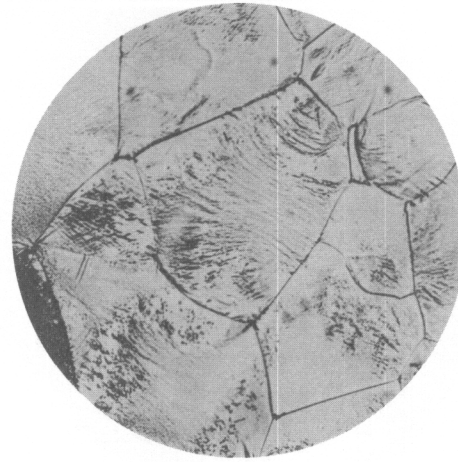


**Fig. 7** Ti-3%Al-8%Cr. Center of  $\frac{1}{2}$ -in. Bar.  
1000°C-20min/W.Q. VHN=280. 100X.

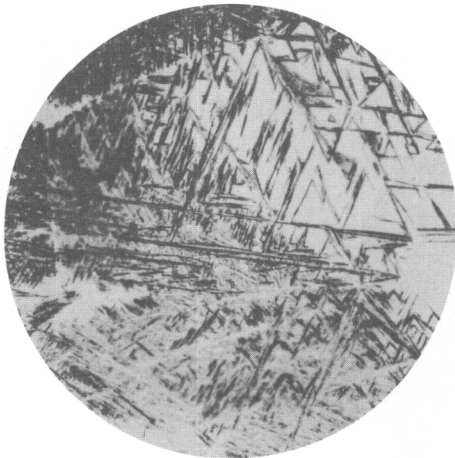


**Fig. 8** Ti-6%Mn. Center of  $\frac{1}{2}$ -in. Bar.  
1000°C-20min/W.Q. VHN=450. 100X.

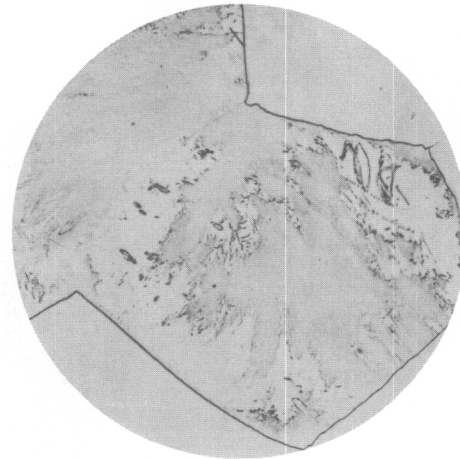
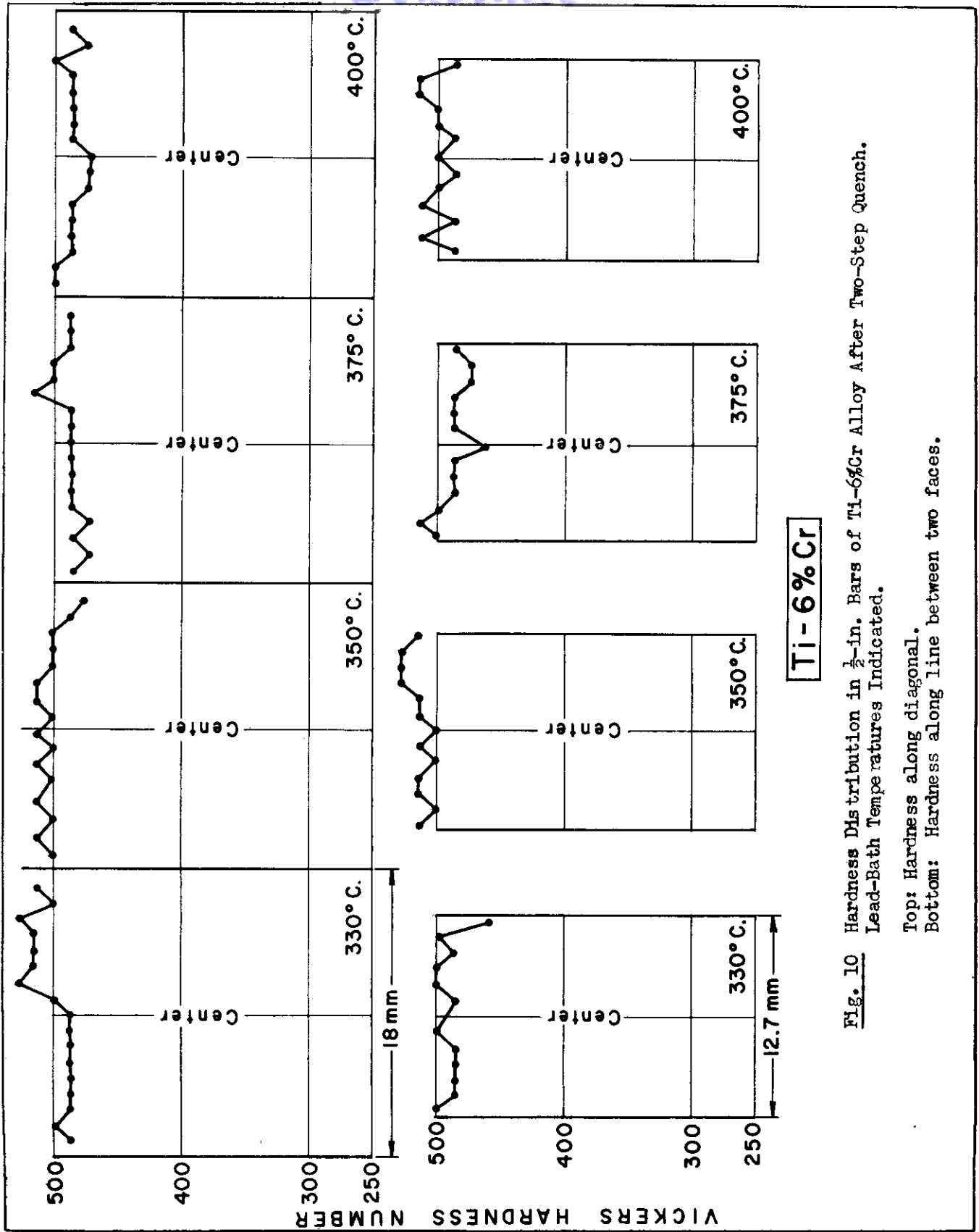


**Fig. 9** Ti-12%Mn. Center of  $\frac{1}{2}$ -in. Bar.  
1000°C-20min/W.Q. VHN=320. 100X.

10 ML. GLYCERINE, 10 ML. CONE HNO<sub>3</sub>, 10 ML. HF, ETCH

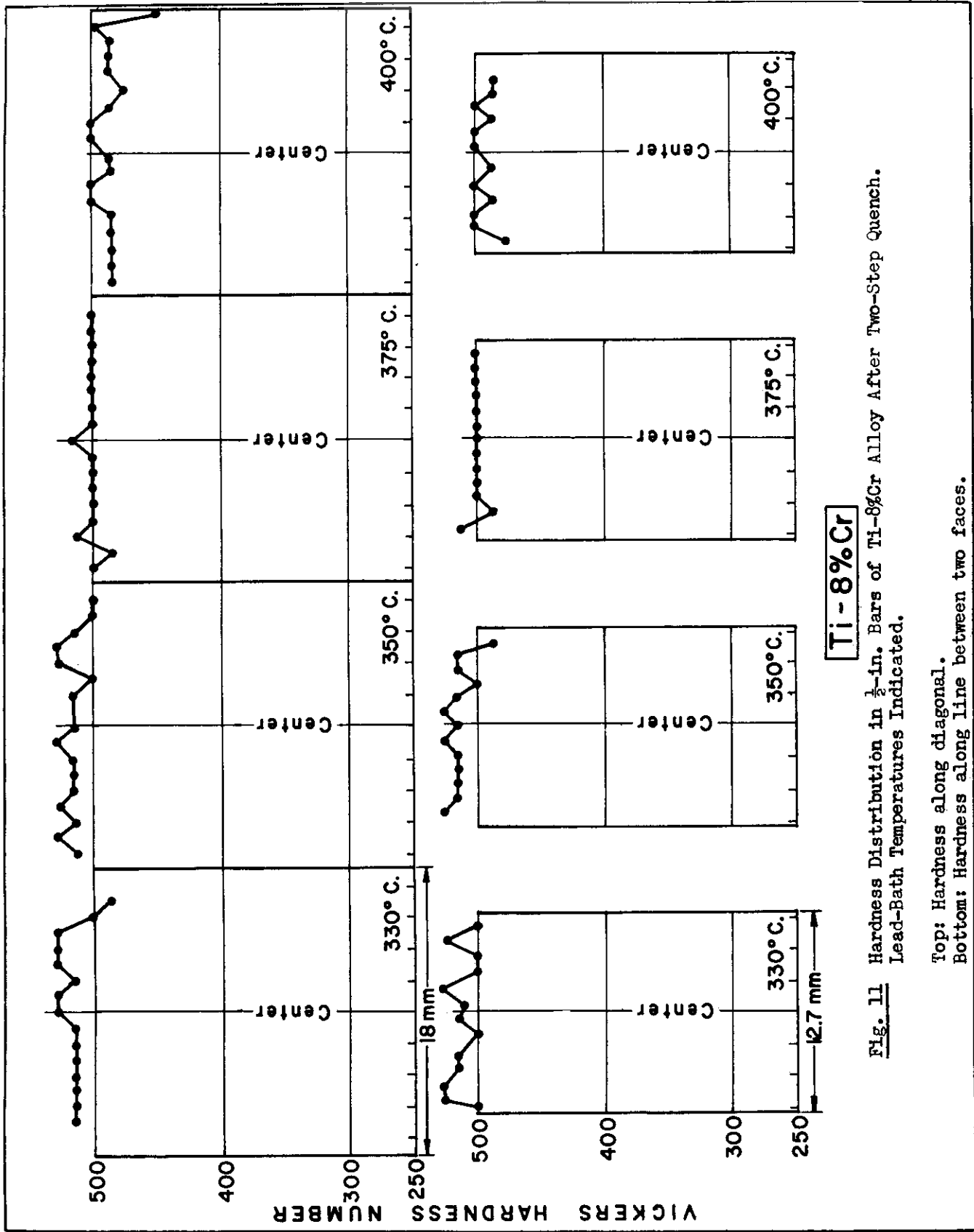
WADC TR54-280

-28



**Fig. 10** Hardness Distribution in  $\frac{1}{2}$ -in. Bars of Ti-6%Cr Alloy After Two-Step Quench. Lead-Bath Temperatures Indicated.

Top: Hardness along diagonal.  
 Bottom: Hardness along line between two faces.



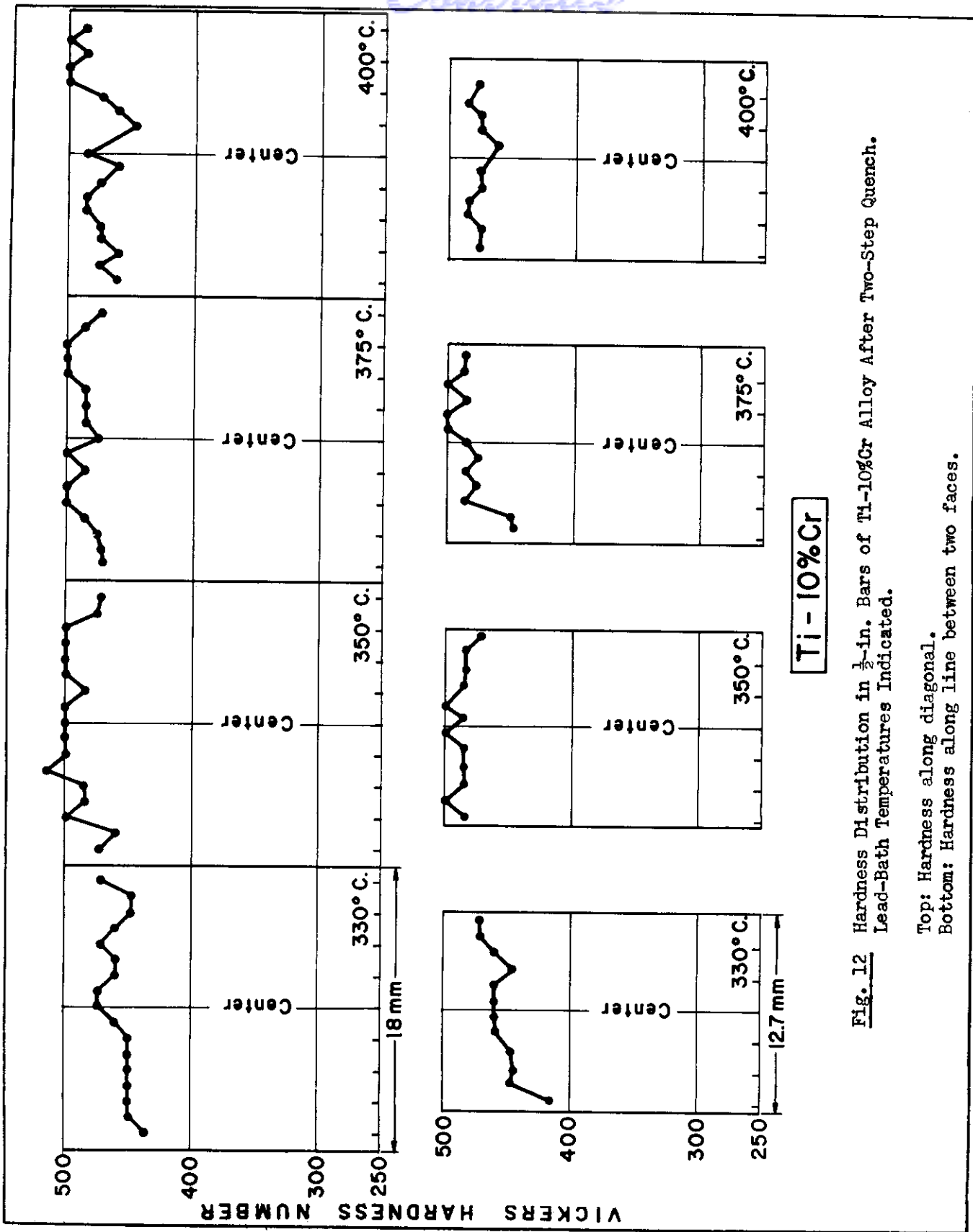
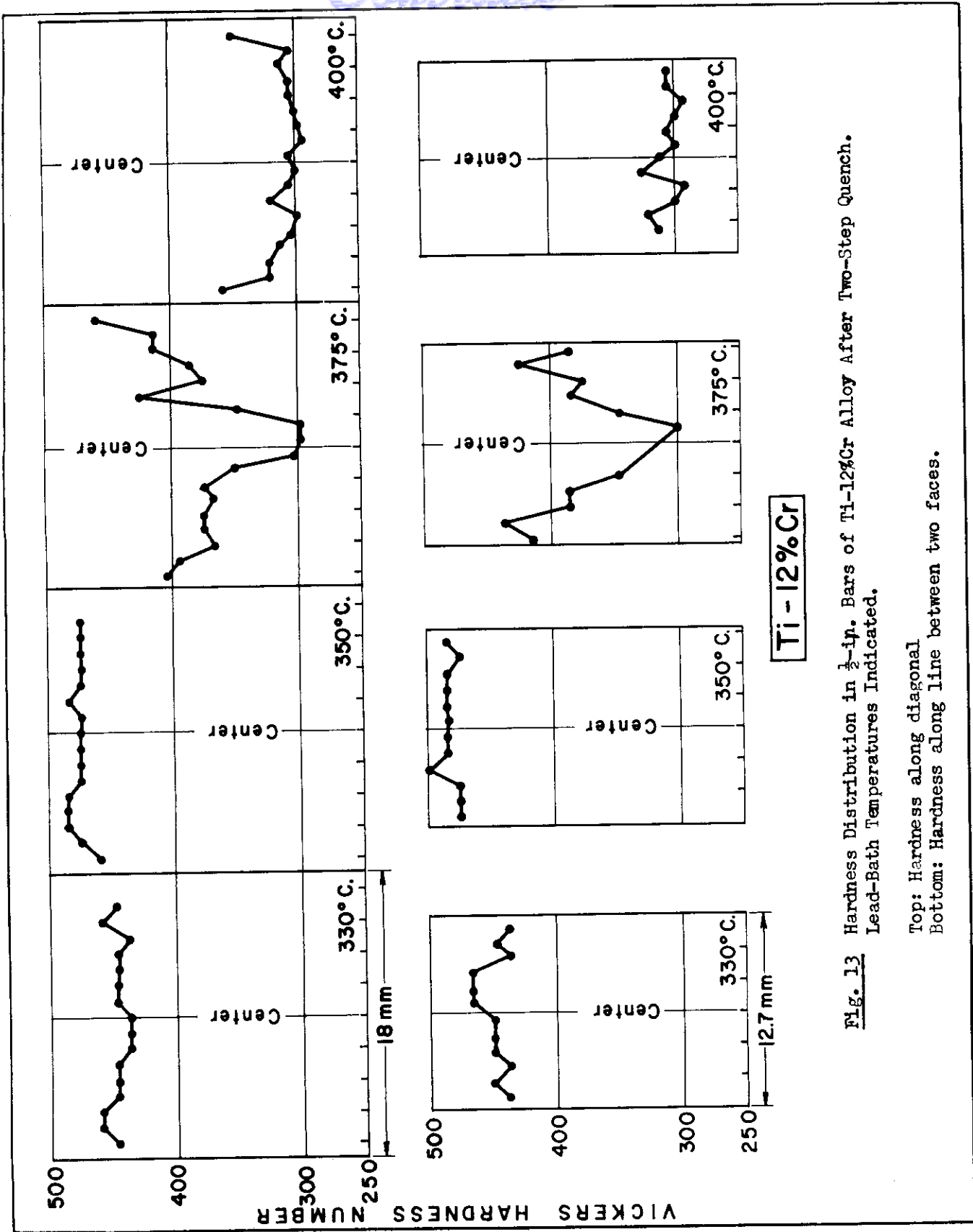


Fig. 12 Hardness Distribution in 1/2-in. Bars of Ti-10%Cr Alloy After Two-Step Quench. Lead-Bath Temperatures Indicated.

Top: Hardness along diagonal.  
Bottom: Hardness along line between two faces.



**Fig. 13** Hardness Distribution in  $\frac{1}{2}$ -in. Bars of Ti-12%Cr Alloy After Two-Step Quench.  
Lead-Bath Temperatures Indicated.

Top: Hardness along diagonal  
Bottom: Hardness along line between two faces.



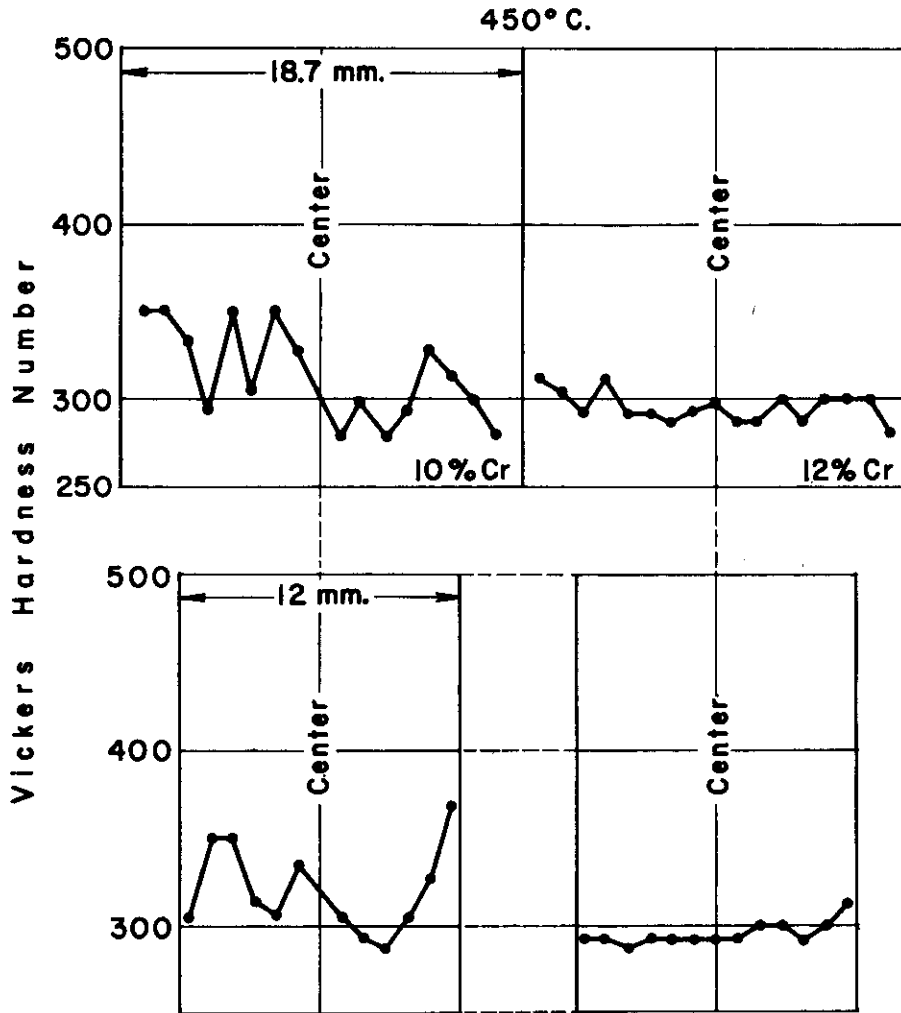
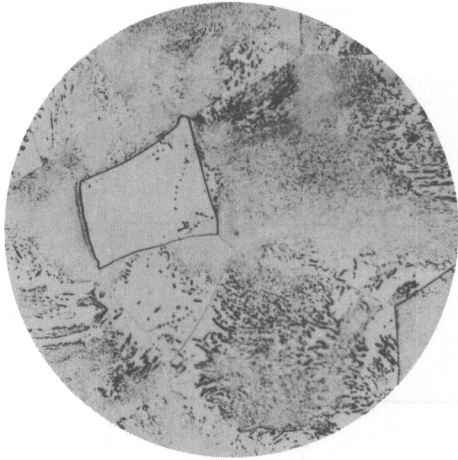


Fig. 14 Hardness Distribution in  $\frac{1}{2}$ -in. Bars of Ti-Cr Alloys of Indicated Composition After Two-Step Quench. Lead-Bath Temperature 450°C.

Top: Hardness along diagonal.

Bottom: Hardness along line between two faces.

# Contrails



**Fig. 15** Ti-10%Cr. Center of  $\frac{1}{2}$ -in. Bar.  
1000°C-20min/375°C-5min/W.Q. VHN=490. 100X.



**Fig. 16** Ti-10%Cr. Center of  $\frac{1}{2}$ -in. Bar.  
1000°C-20min/400°C-5min/W.Q. VHN=475. 100X

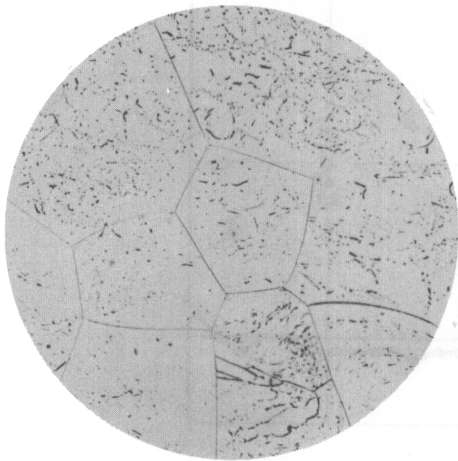


**Fig. 17** Ti-12%Cr. Outer Layer of  $\frac{1}{2}$ -in. Bar.  
1000°C-20min/400°C-5min/W.Q. VHN=360. 100X.



**Fig. 18** Ti-12%Cr. Center of  $\frac{1}{2}$ -in. Bar.  
1000°C-20min/400°C-5min/W.Q. VHN=300. 100X.

10 ML. GLYCERINE, 10 ML. CONC.  $\text{HNO}_3$ , 10 ML. HF, ETCH  
WADC TR54-280

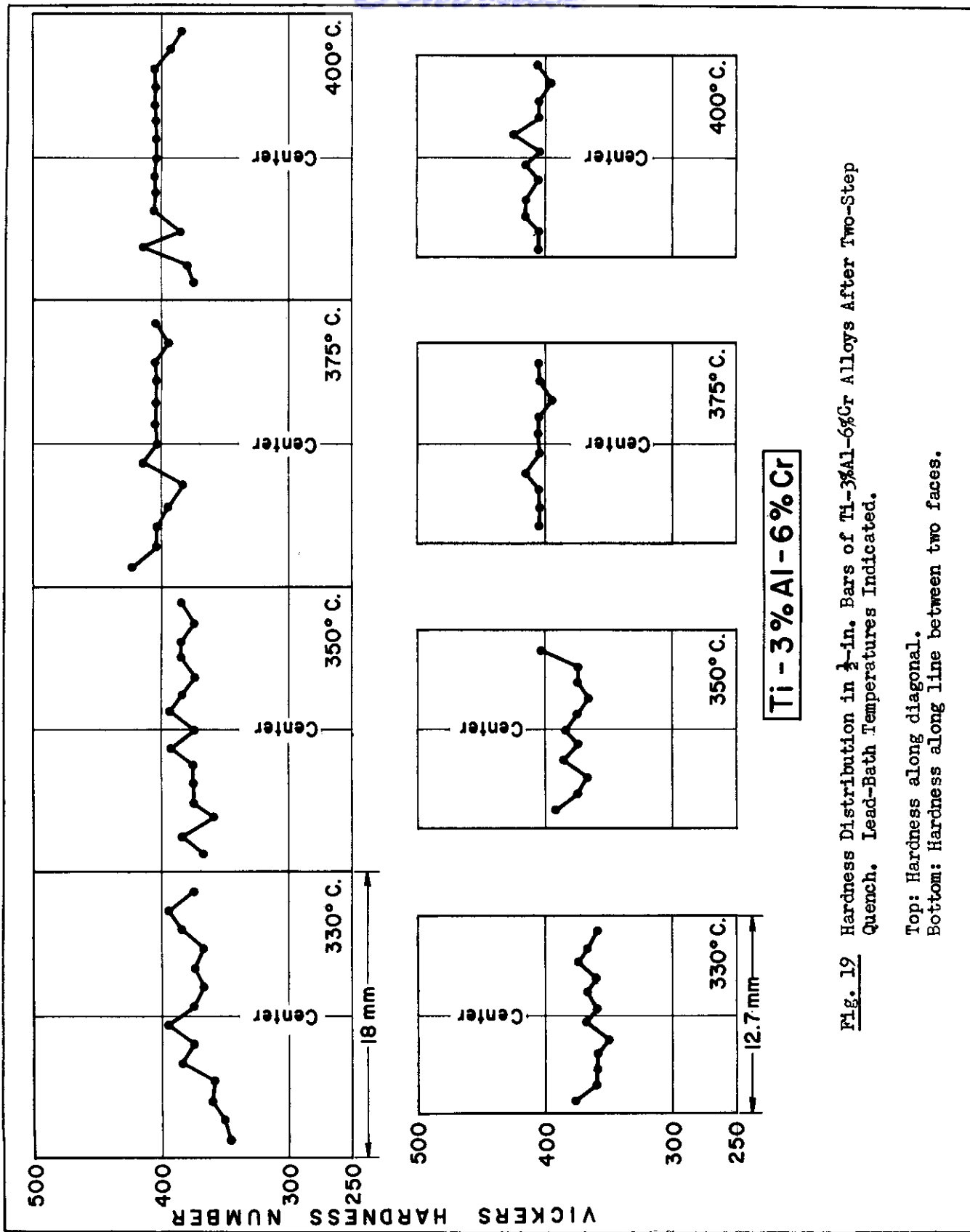


**Fig. 19** Hardness Distribution in  $\frac{1}{2}$ -in. Bars of Ti-3%Al-6%Cr Alloys After Two-Step Quench. Lead-Bath Temperatures Indicated.

Top: Hardness along diagonal.  
 Bottom: Hardness along line between two faces.

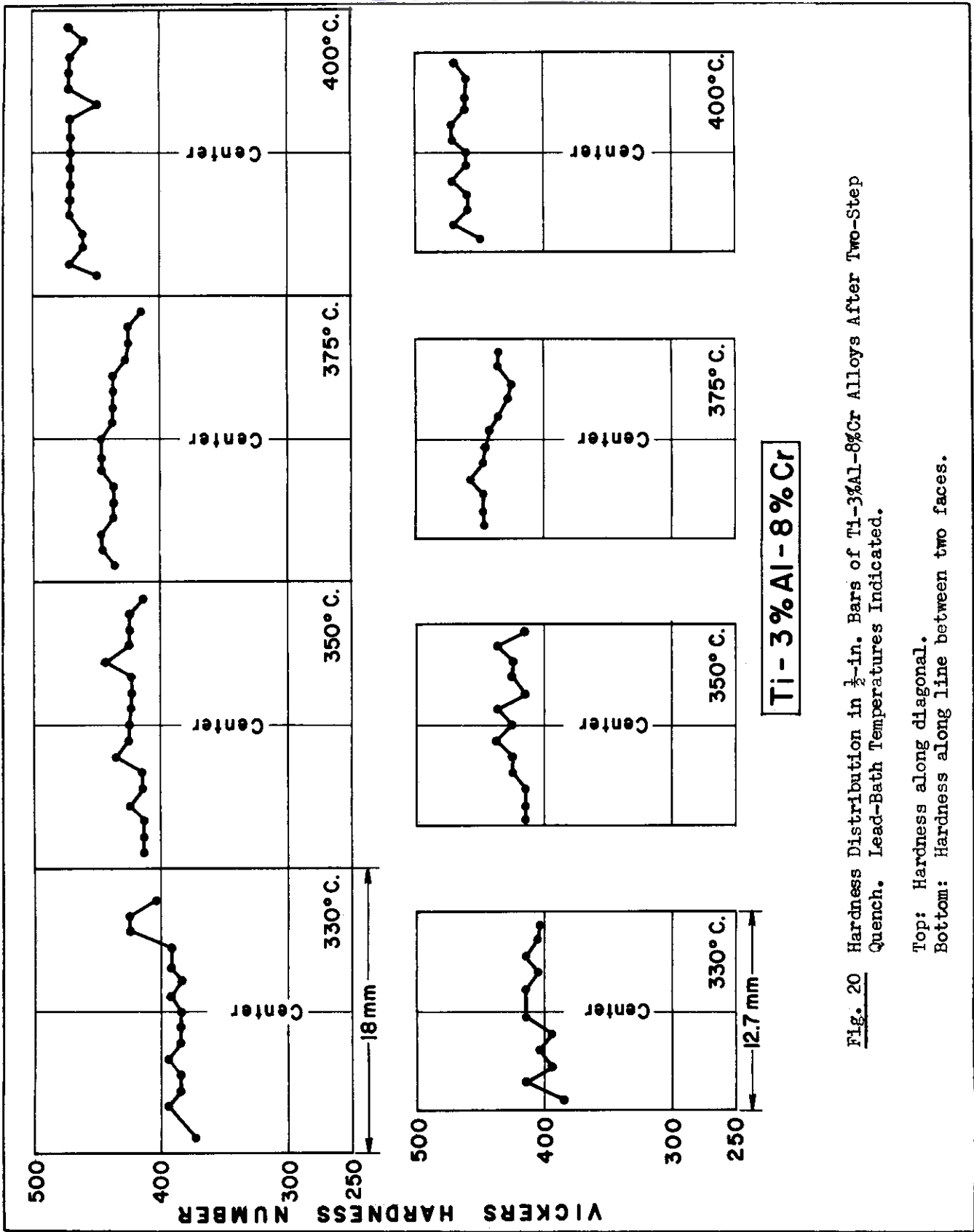


Fig. 20 Hardness Distribution in  $\frac{1}{2}$ -in. Bars of Ti-3%Al-8%Cr Alloys After Two-Step Quench. Lead-Bath Temperatures Indicated.

Top: Hardness along diagonal.  
 Bottom: Hardness along line between two faces.

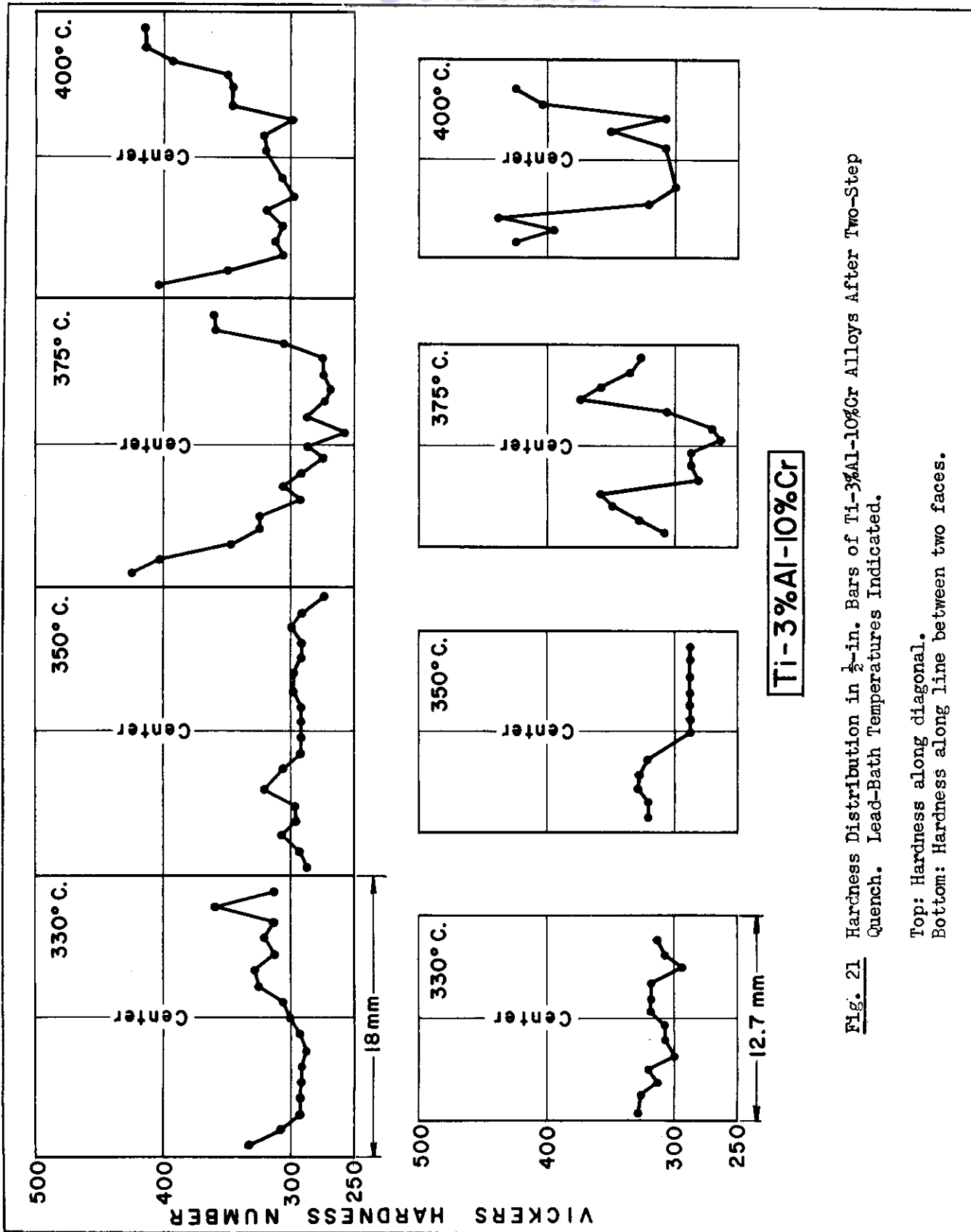
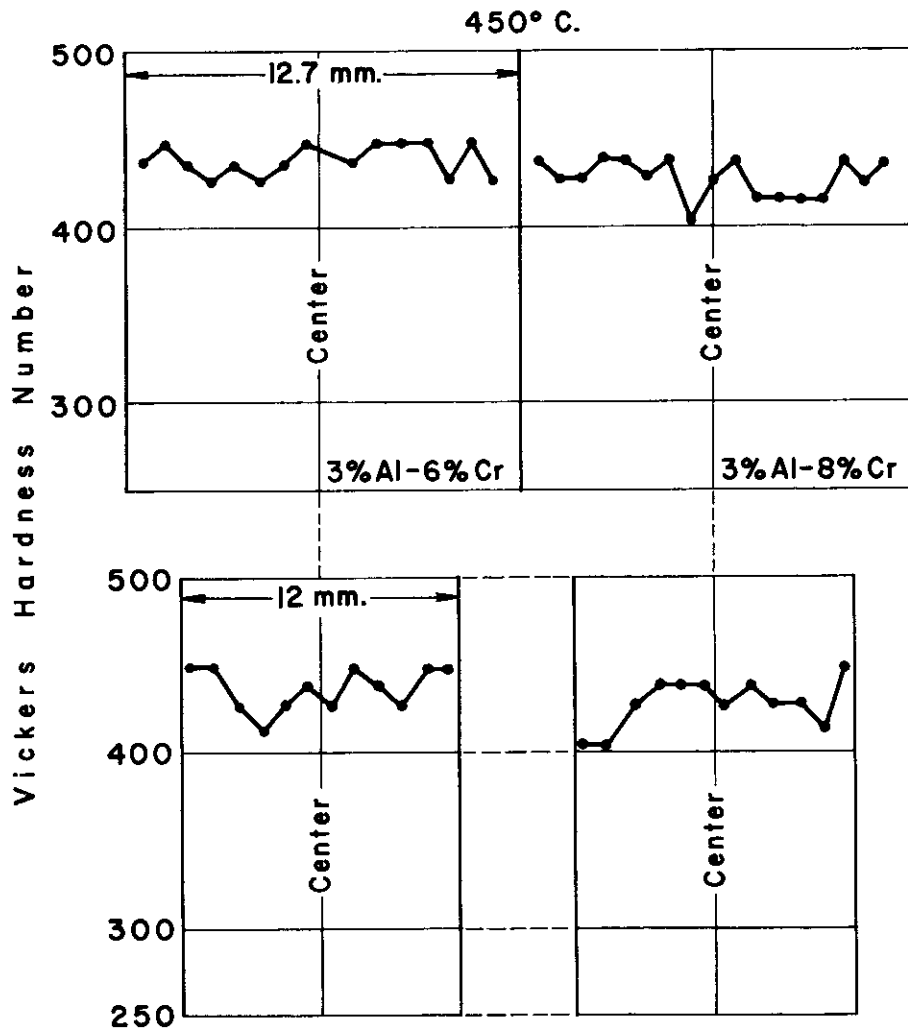


Fig. 21 Hardness Distribution in  $\frac{1}{2}$ -in. Bars of Ti-3%Al-10%Cr Alloys After Two-Step Quench. Lead-Bath Temperatures Indicated.

Top: Hardness along diagonal.  
 Bottom: Hardness along line between two faces.



**Fig. 22** Hardness Distribution in  $\frac{1}{2}$ -in. Bars of Ti-3%Al-Cr Alloys of Indicated Compositions After Two-Step Quench. Lead-Bath Temperature 450°C.

Top: Hardness along diagonal.

Bottom: Hardness along line between two faces.

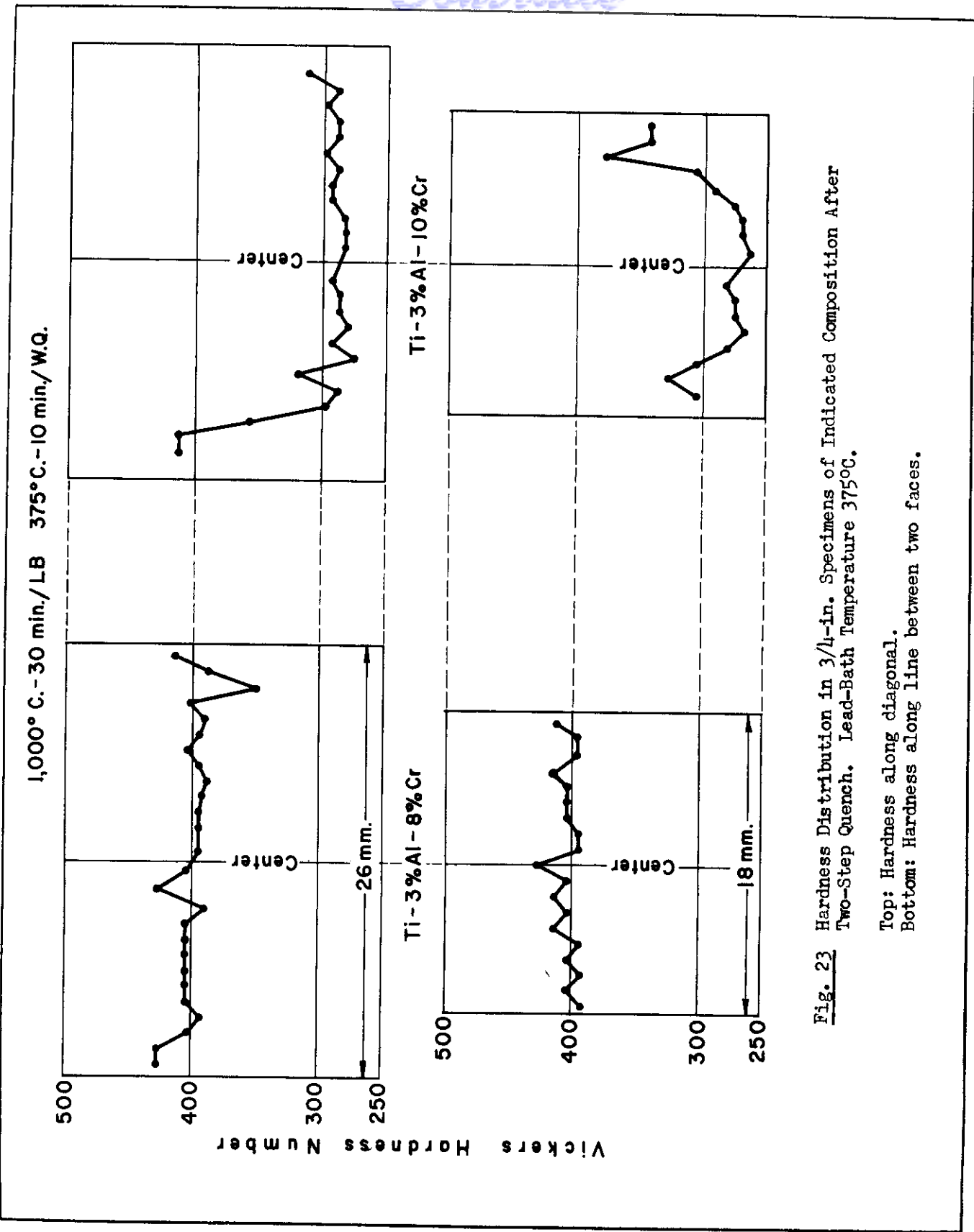


Fig. 23 Hardness Distribution in 3/4-in. Specimens of Indicated Composition After Two-Step Quench. Lead-Bath Temperature 375°C.

Top: Hardness along diagonal.  
Bottom: Hardness along line between two faces.

# Contrails

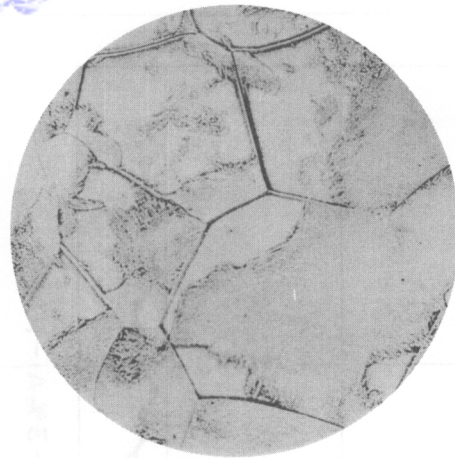
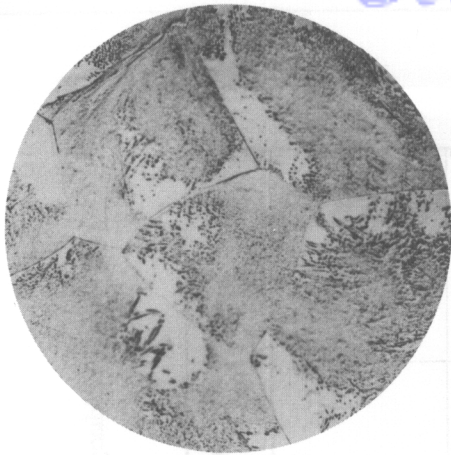


Fig. 24 Ti-3%Al-8%Cr. Center of  $\frac{1}{2}$ -in. Bar.  $1000^{\circ}\text{C}$ -30min/ $400^{\circ}\text{C}$ -5min/W.Q. VHN=475. 100X.

Fig. 25 Ti-3%Al-8%Cr. Center of  $\frac{1}{2}$ -in. Bar.  $1000^{\circ}\text{C}$ -30min/ $450^{\circ}\text{C}$ -5min/W.Q. VHN=425. 100X.

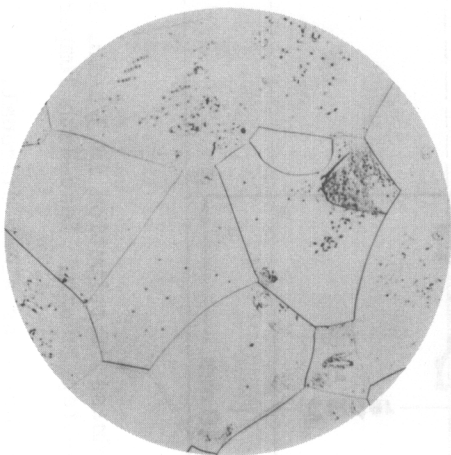
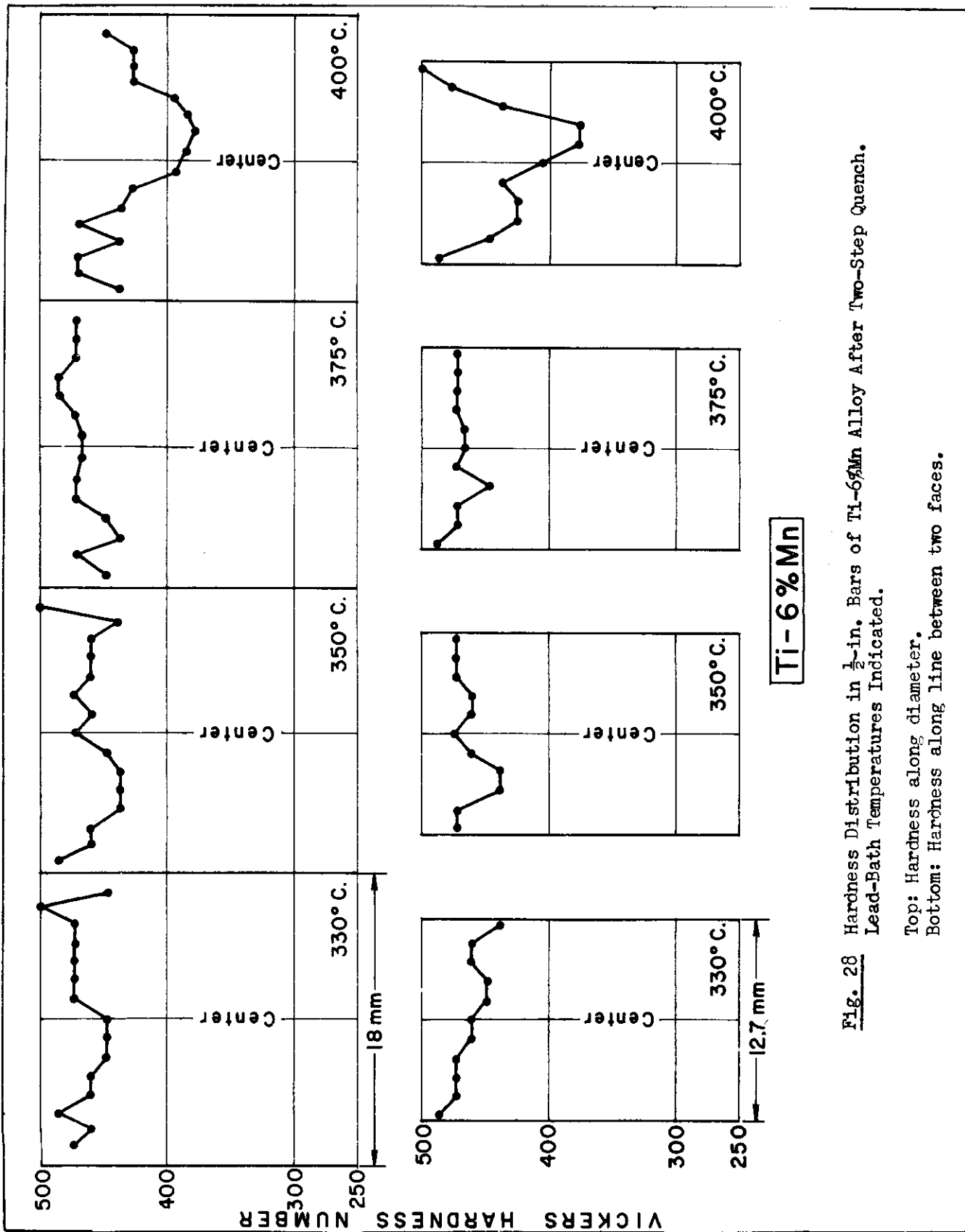


Fig. 26 Ti-3%Al-8%Cr. Outer Layer of  $\frac{1}{2}$ -in. Bar  $1000^{\circ}\text{C}$ -20min/ $400^{\circ}\text{C}$ -5min/W.Q. VHN=415.

Fig. 27 Ti-3%Al-10%Cr. Center of  $\frac{1}{2}$ -in. Bar  $1000^{\circ}\text{C}$ -20min/ $400^{\circ}\text{C}$ -5min/W.Q. VHN=320. 100X

10 ML. GLYCERINE, 10 ML. CONE  $\text{HNO}_3$ , 10 ML. HF, ETCH  
WADC TR 54-280





**Fig. 28** Hardness Distribution in  $\frac{1}{2}$ -in. Bars of Ti-6%Mn Alloy After Two-Step Quench. Lead-Bath Temperatures Indicated.

Top: Hardness along diameter.

Bottom: Hardness along line between two faces.

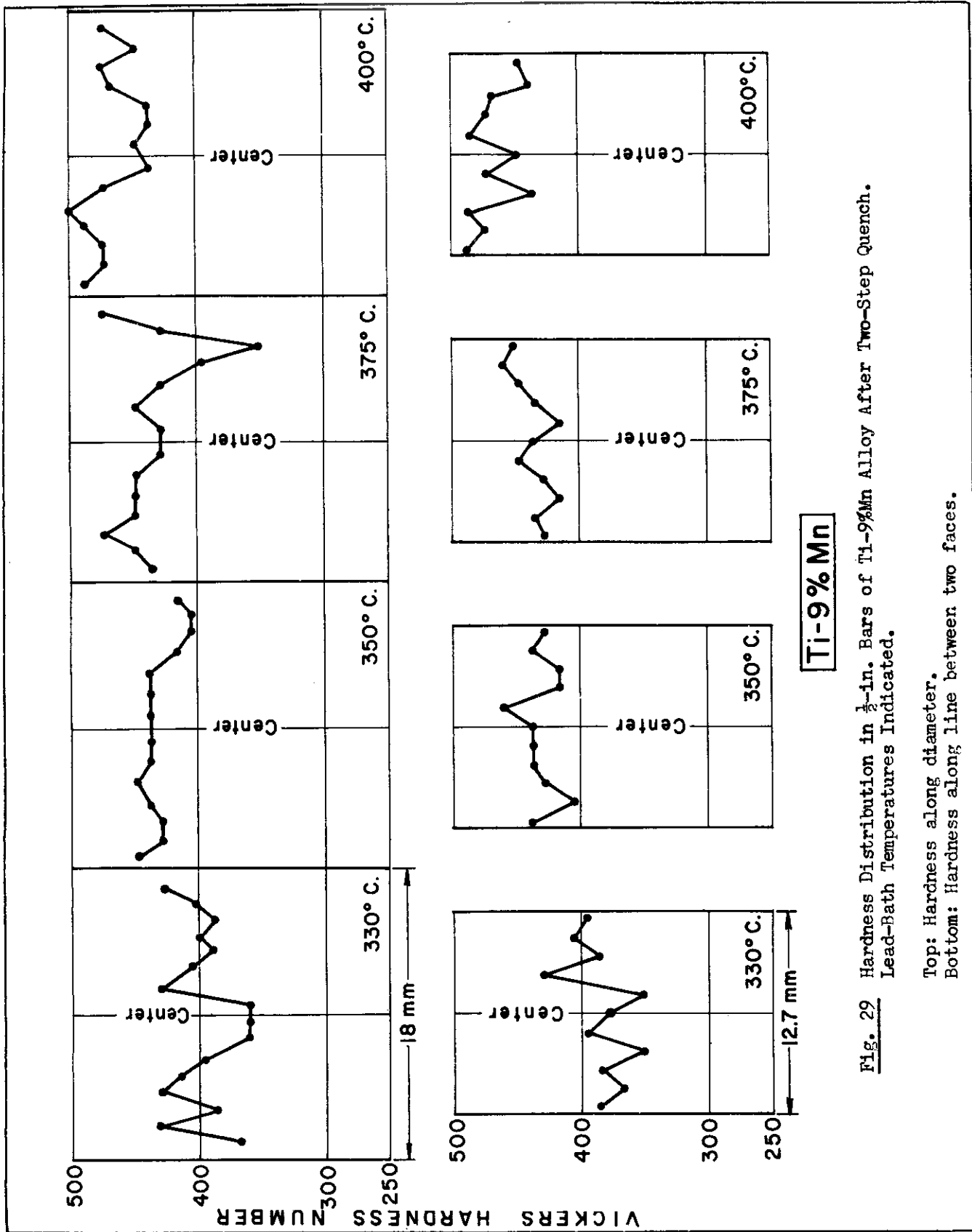
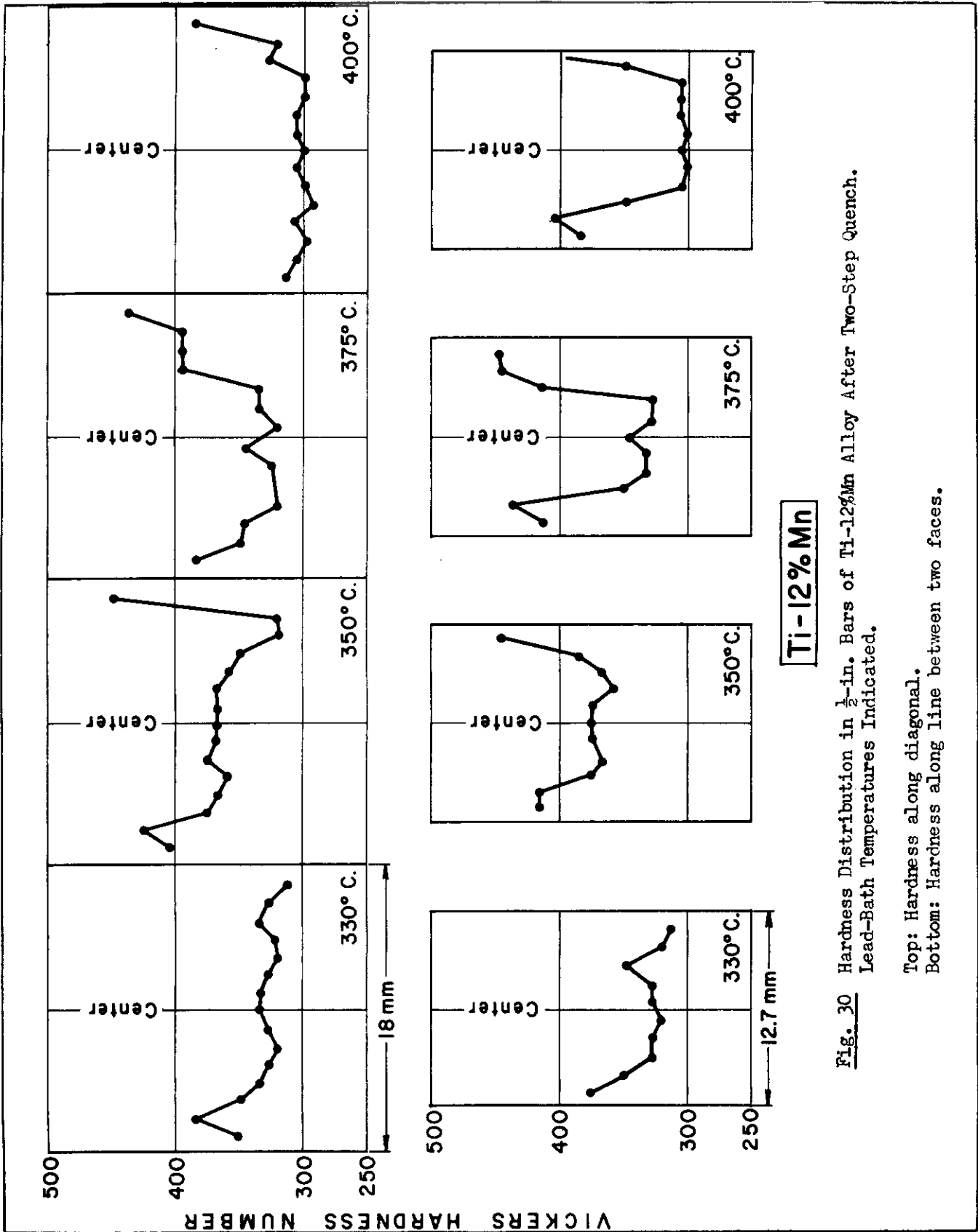


Fig. 29 Hardness Distribution in  $\frac{1}{2}$ -in. Bars of Ti-9%Mn Alloy After Two-Step Quench. Lead-Bath Temperatures Indicated.

Top: Hardness along diameter.

Bottom: Hardness along line between two faces.



**Fig. 30** Hardness Distribution in  $\frac{1}{2}$ -in. Bars of Ti-12%Mn Alloy After Two-Step Quench. Lead-Bath Temperatures Indicated.

Top: Hardness along diagonal.  
 Bottom: Hardness along line between two faces.

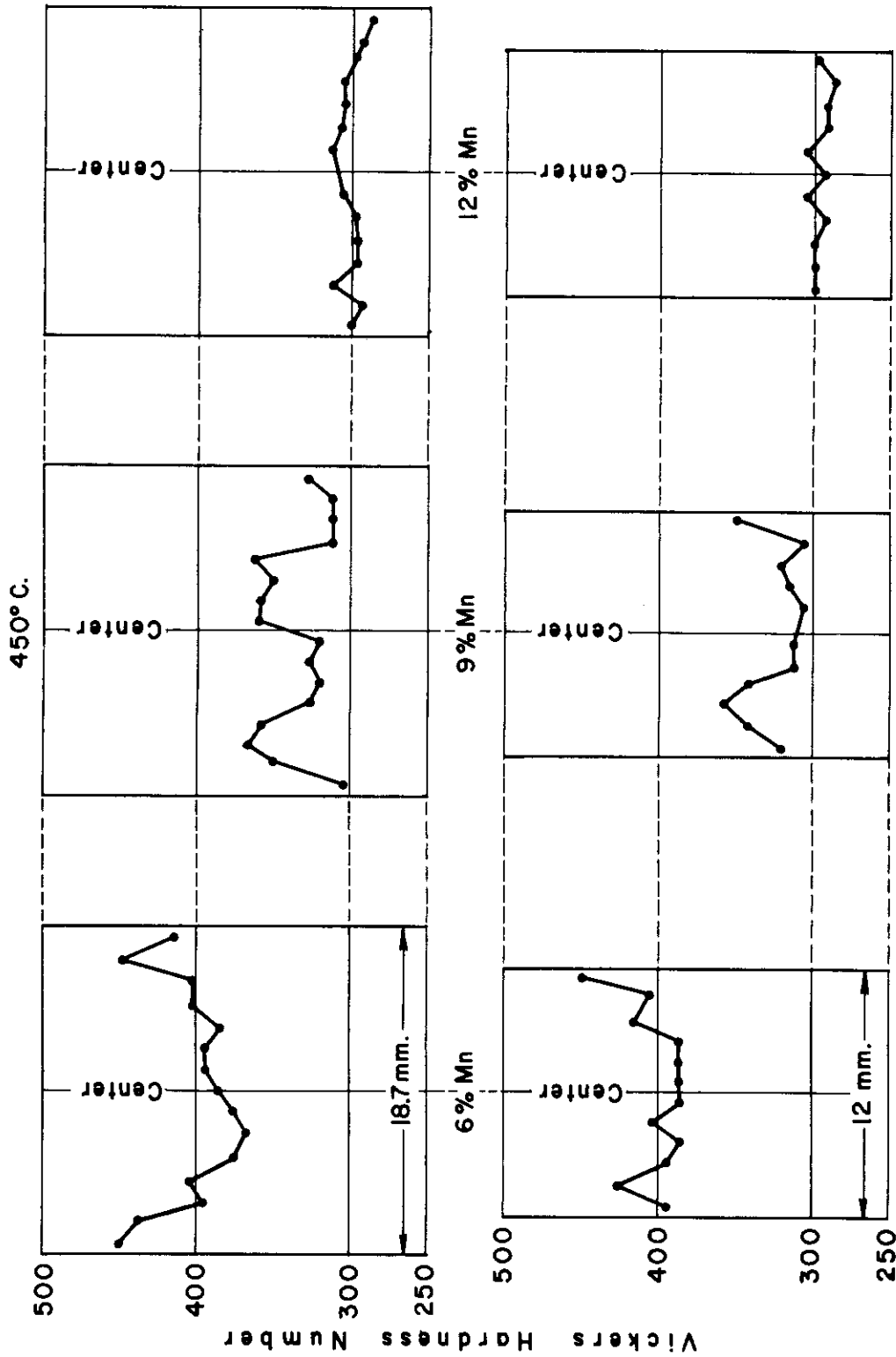
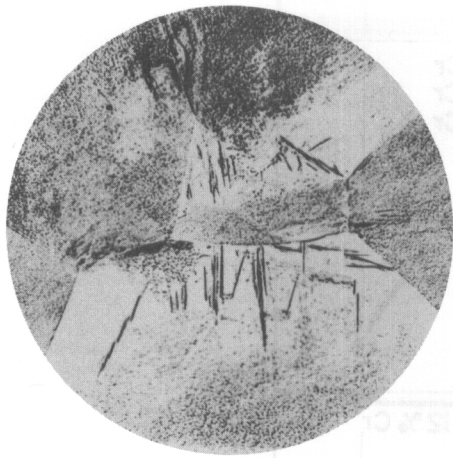


Fig. 31 Hardness Distribution in 1/2-in. Bars of Ti-Mn Alloys of Indicated Composition After Two-Step Quench. Lead-Bath Temperature 450°C.

Top: Hardness along diagonal.  
 Bottom: Hardness along line between two faces.

# Contrails



**Fig. 32** Ti-6%Mn. Center of  $\frac{1}{2}$ -in. Bar.  
1000°C-20min/400°C-5min/W.Q. VHN=385. 100X.

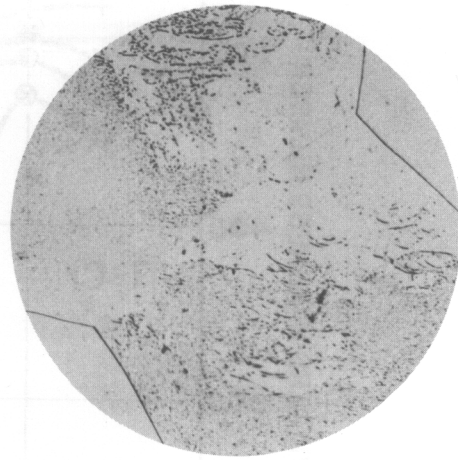


**Fig. 33** Ti-9%Mn. Center of  $\frac{1}{2}$ -in. Bar.  
1000°C-20min/400°C-5min/W.Q. VHN=450. 100X.

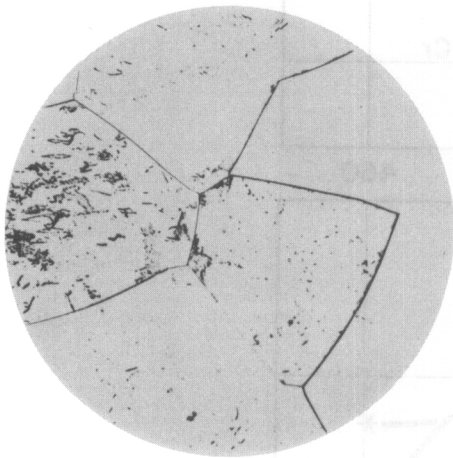


**Fig. 34** Ti-12%Mn. Outer Layer of  $\frac{1}{2}$ -in. Bar.  
1000°C-20min/400°C-5min/W.Q. VHN=380. 100X.

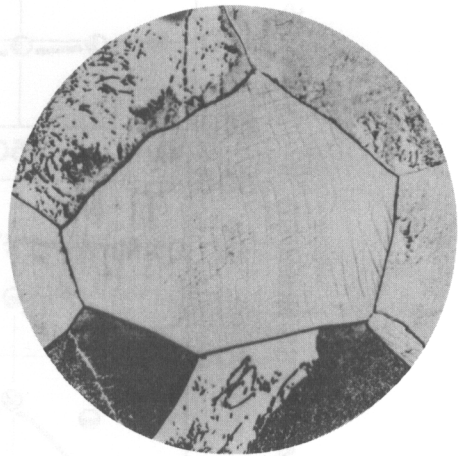


**Fig. 35** Ti-12%Mn. Center of  $\frac{1}{2}$ -in. Bar.  
1000°C-20min/400°C-5min/W.Q. VHN=305. 100X.

10 ML. GLYCERINE, 10 ML. CONE  $\text{HNO}_3$ , 10 ML.  $\text{HF}$ , ETCH

WADC TR54-280

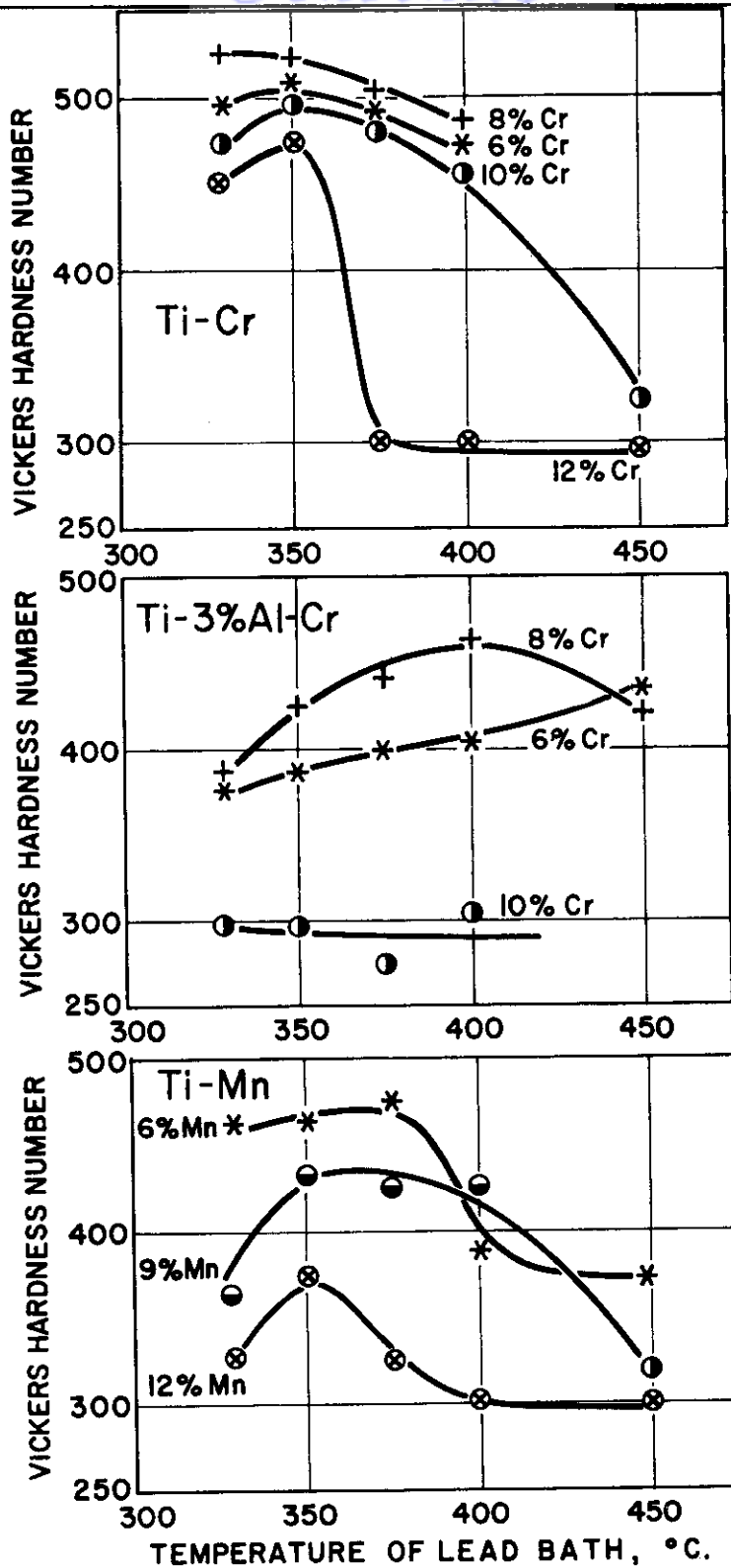


Fig. 36 Hardness in the Center of  $\frac{1}{2}$ -in. Bars After Two-Step Quench versus temperature of the First Quench.

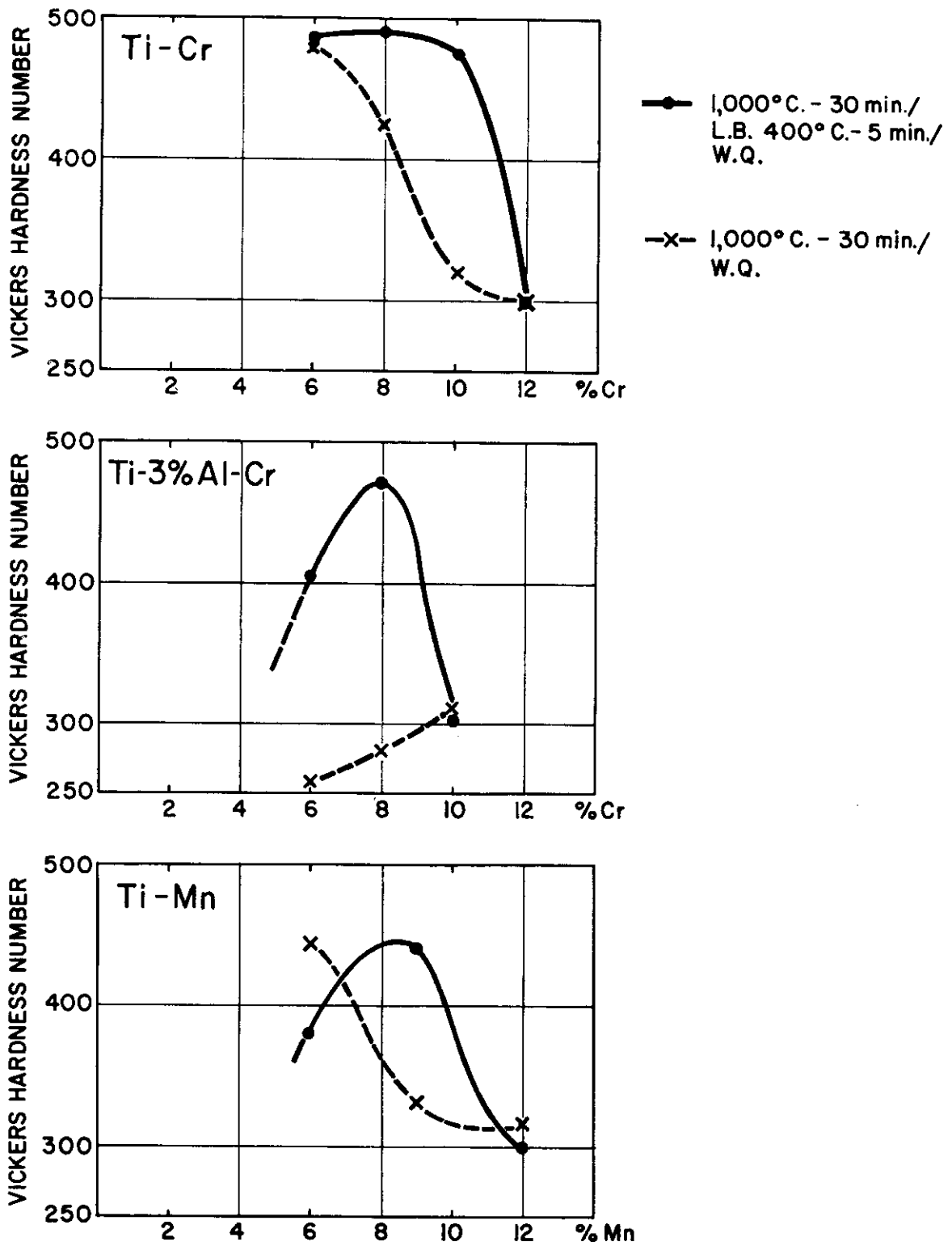


Fig. 37 Effect of Compositions on Hardness in the Center of  $\frac{1}{2}$ -in. Rods After Single and Two-Step Quenching.

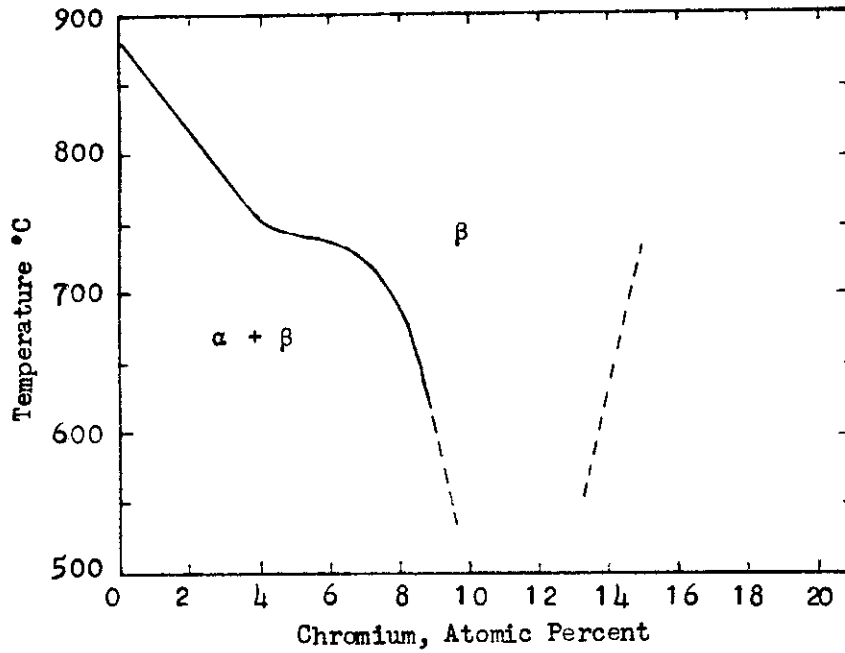


Fig. 38 The Titanium-Chromium Phase Diagram.  
(According to M. K. McQuillan)



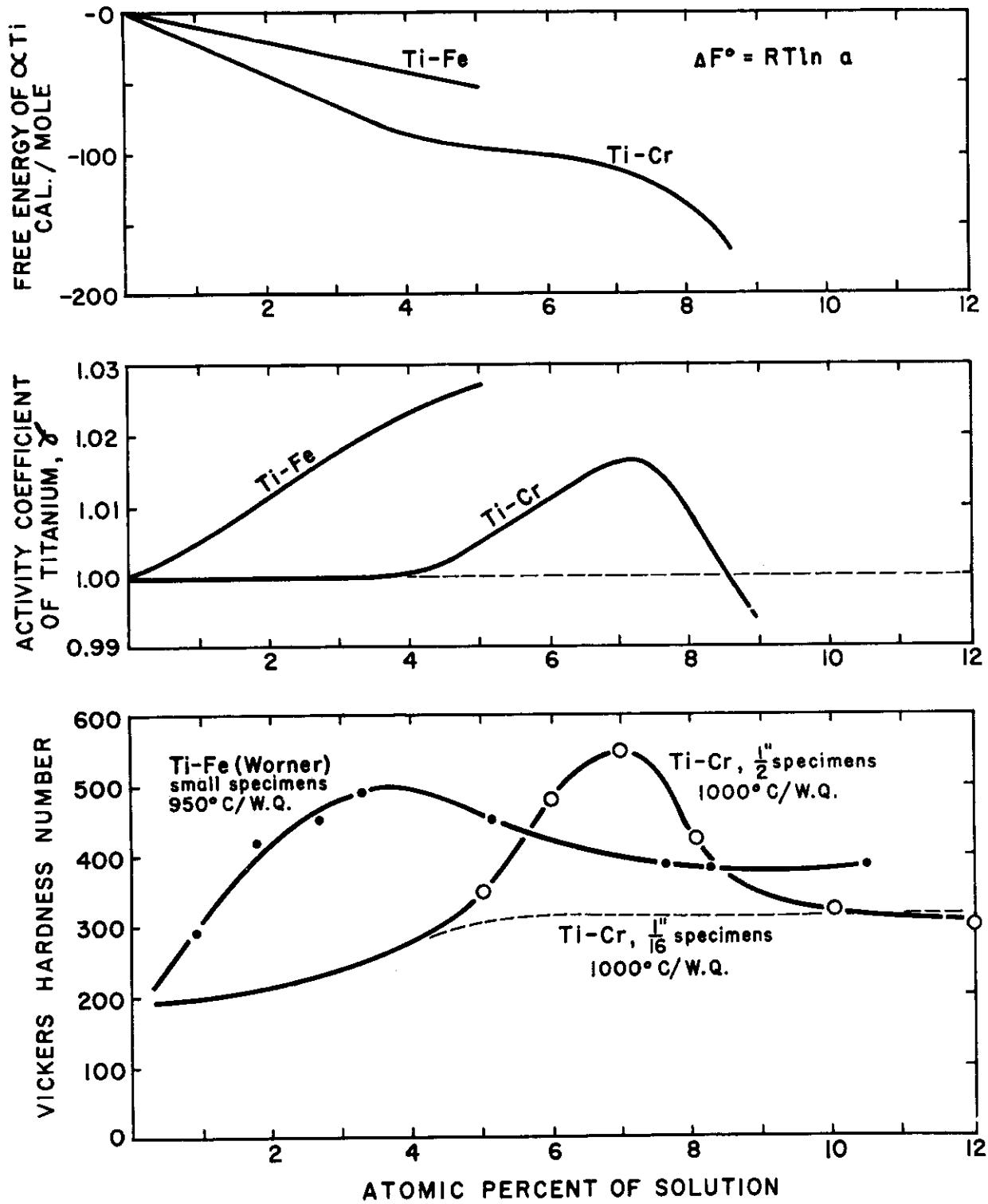


Fig. 39 Free Energy and Activity Coefficient of Titanium, and Hardness of Water-quenched Specimens as a Function of the Solute Content in Ti-Cr and Ti-Fe Alloys.

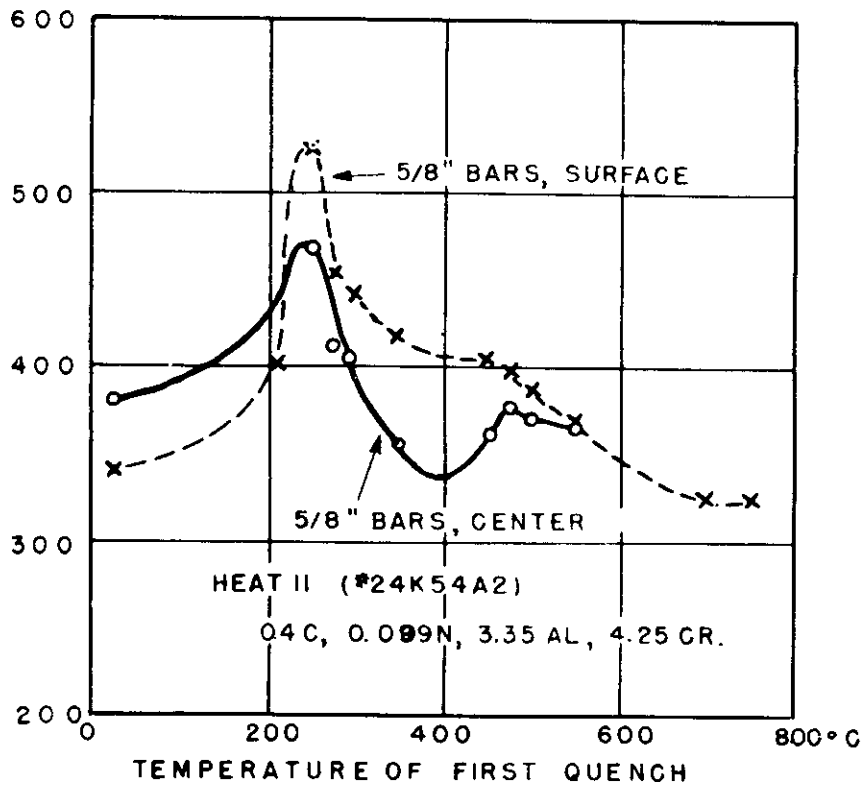
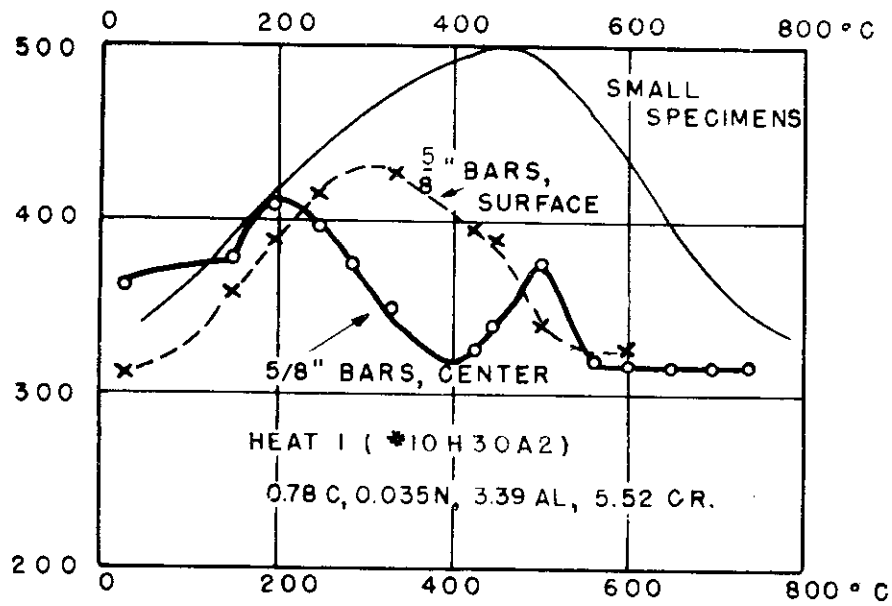


Fig. 40 Hardness in the Center and Outer Zone of 5/8-in. Rounds, as a Function of the Temperature of the First Quench.

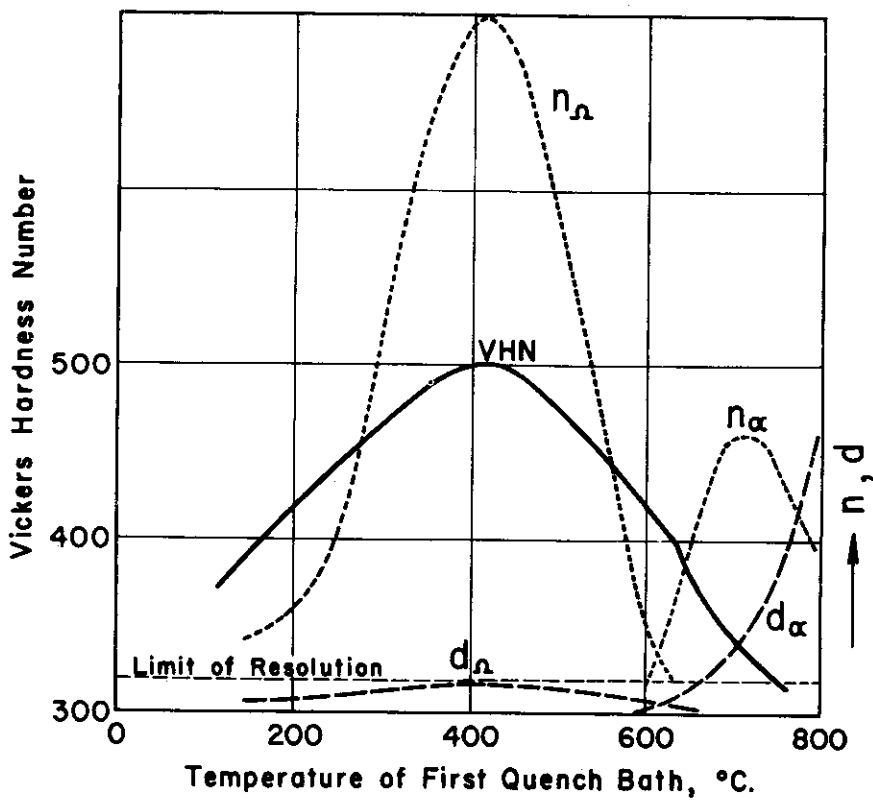
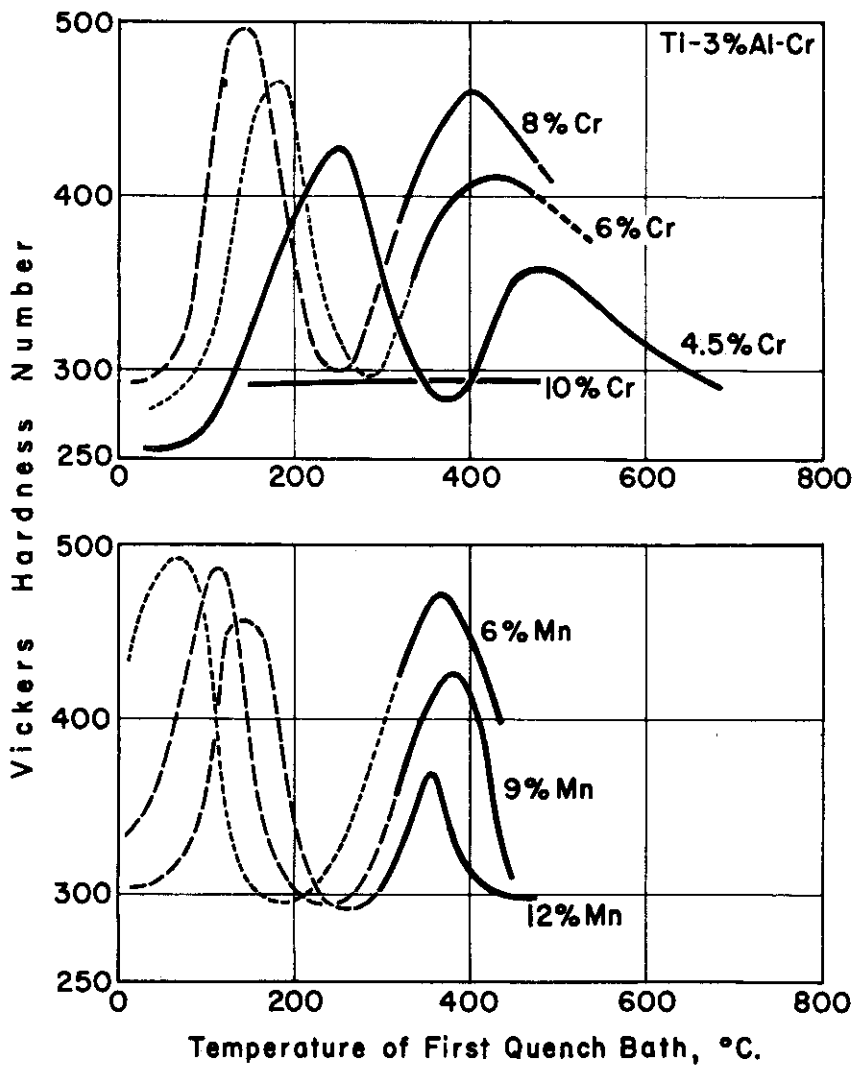


Fig. 41 Hardness (VHN), Diameter of Particles ( $d_{\Omega}$  and  $d_{\alpha}$ ), and Density of Nucleated Particles ( $n_{\Omega}$  and  $n_{\alpha}$ ) as Functions of the Temperatures of the First Quench.



**Fig. 42** Hypothetical Hardness Values in the Core of  $\frac{1}{2}$ -in. Rods After Two-Step Quench as a Function of the First Quench Temperature for Alloys of the Ti-3%Al-Cr and Ti-Mn Series. (Experimentally Observed Values are Drawn as Solid Curves.)